Compressive time-lapse seismic monitoring of carbon storage and sequestration with the joint recovery model

Ziyi Yin, Mathias Louboutin, Philipp A. Witte*, and Felix J. Herrmann




SLIM
Georgia Institute of Technology

* Microsoft Research

Georgia Tech

Carbon capture and storage
Sleipner project

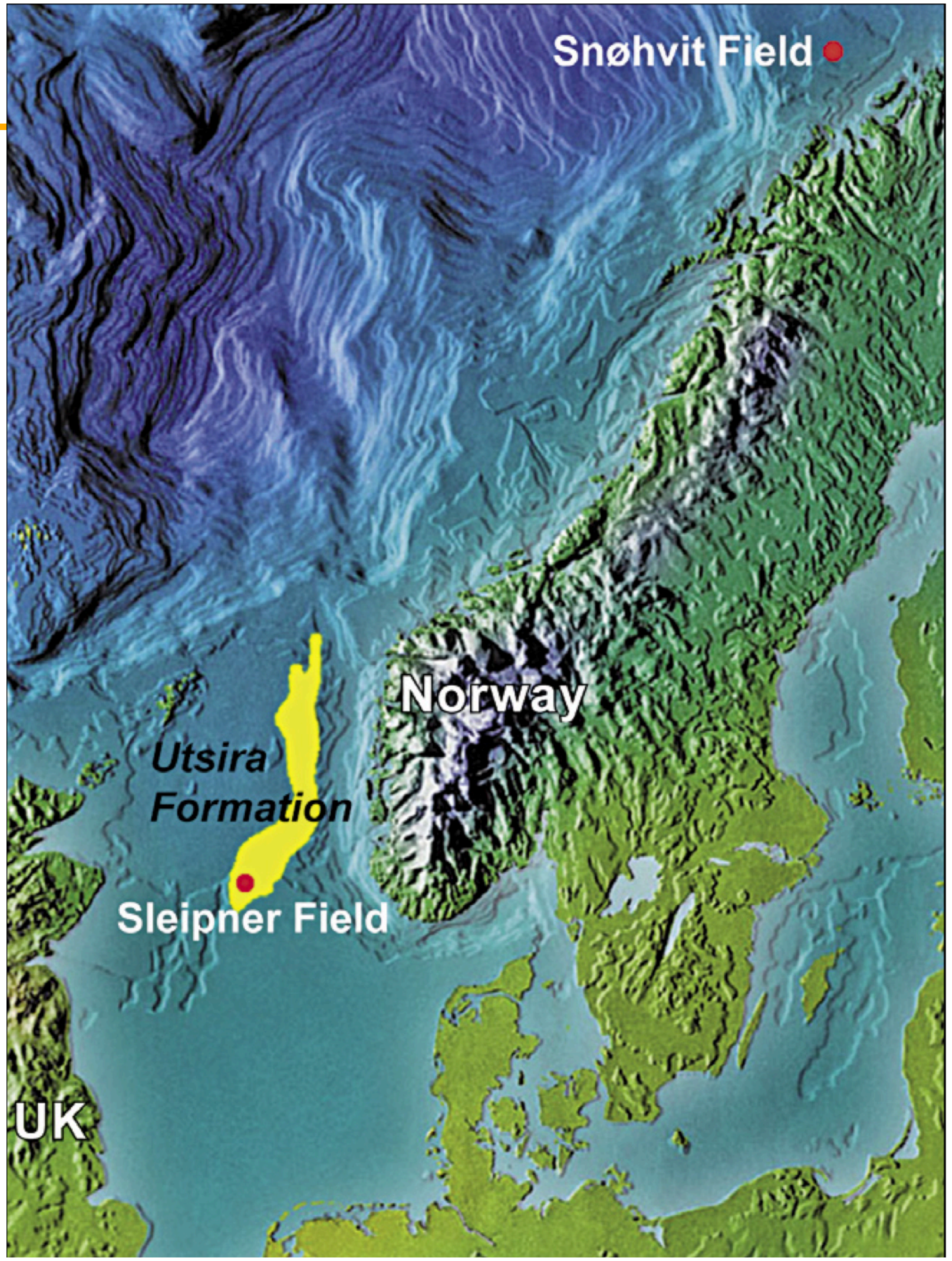

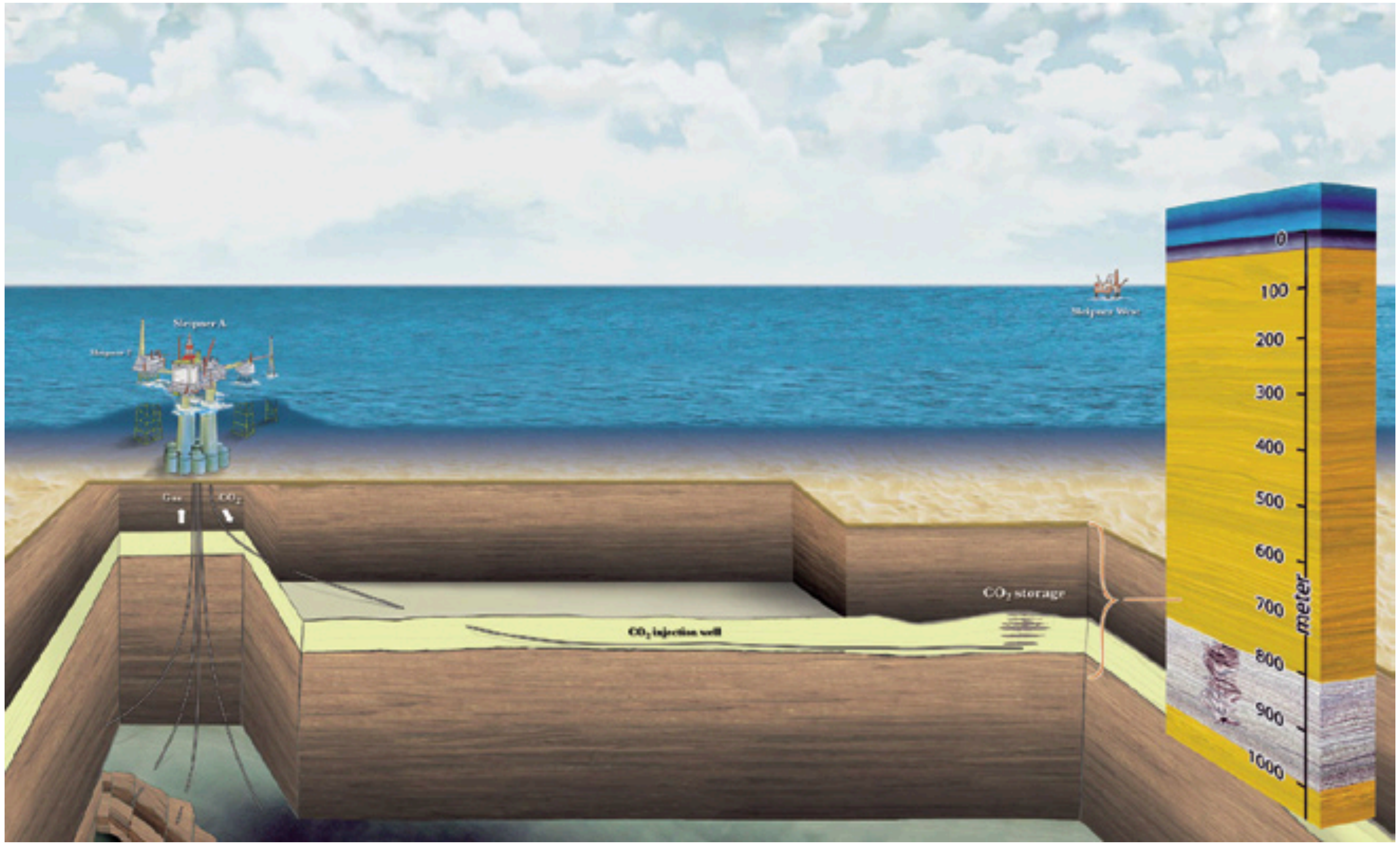

Arts, R. J., et al. "Ten years' experience of monitoring CO2 injection in the Utsira Sand at Sleipner, offshore Norway." *First break* 26.1 (2008).

Seismic response
Sleipner project

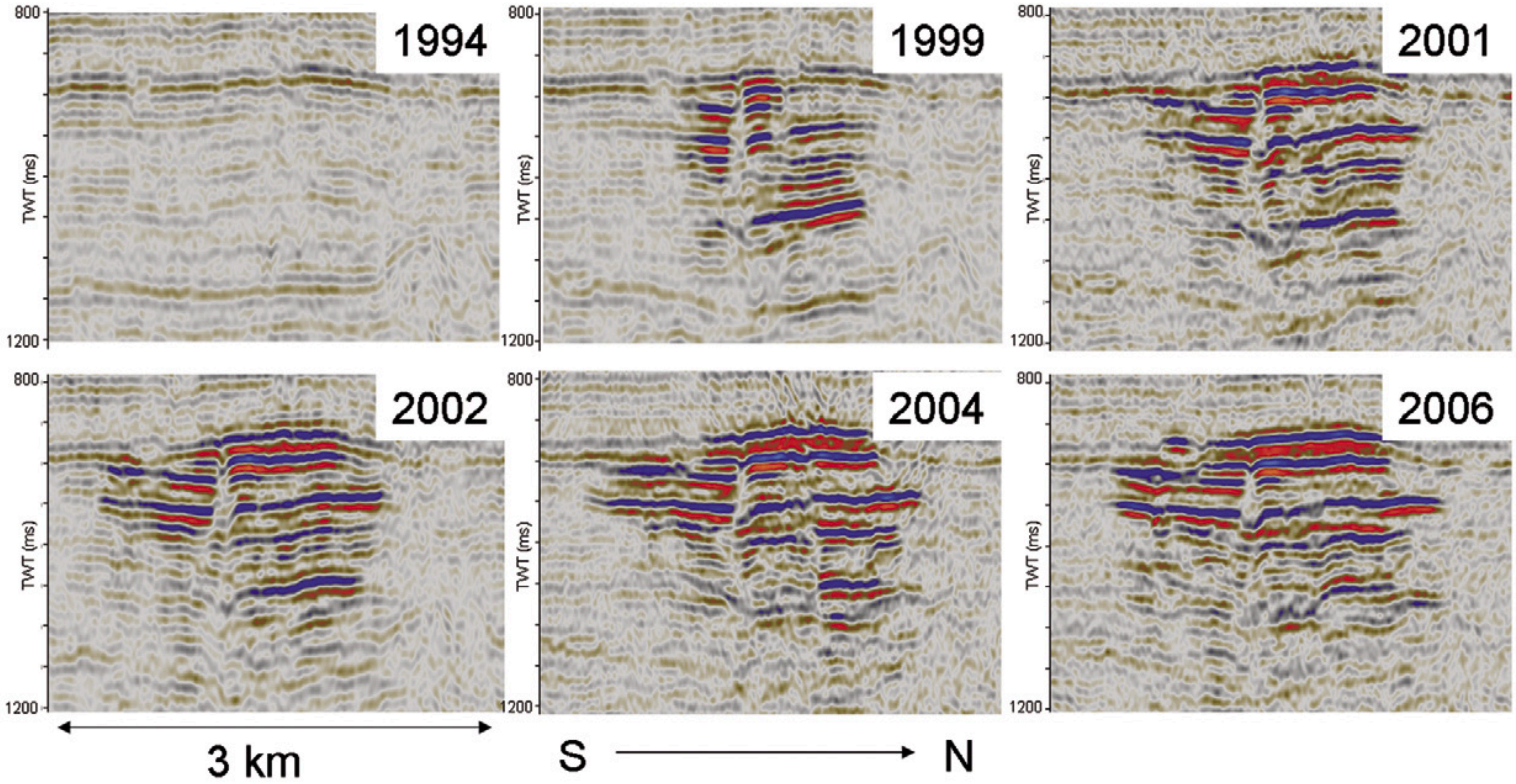

Arts, R. J., et al. "Ten years' experience of monitoring CO2 injection in the Utsira Sand at Sleipner, offshore Norway." *First break* 26.1 (2008).

Motivation

seismic monitoring of CCS

Seismic imaging of CO_2 plume in a realistic setting to

- mitigate risk of CO_2 leakage by early detection
- lower cost of seismic monitoring
- develop publicly available open source software framework

Build industry-scale reproducible system to

- design & evaluate sensitivity of seismic monitoring for CCS
- accelerate rate of innovation

Establish a workflow

Workflow

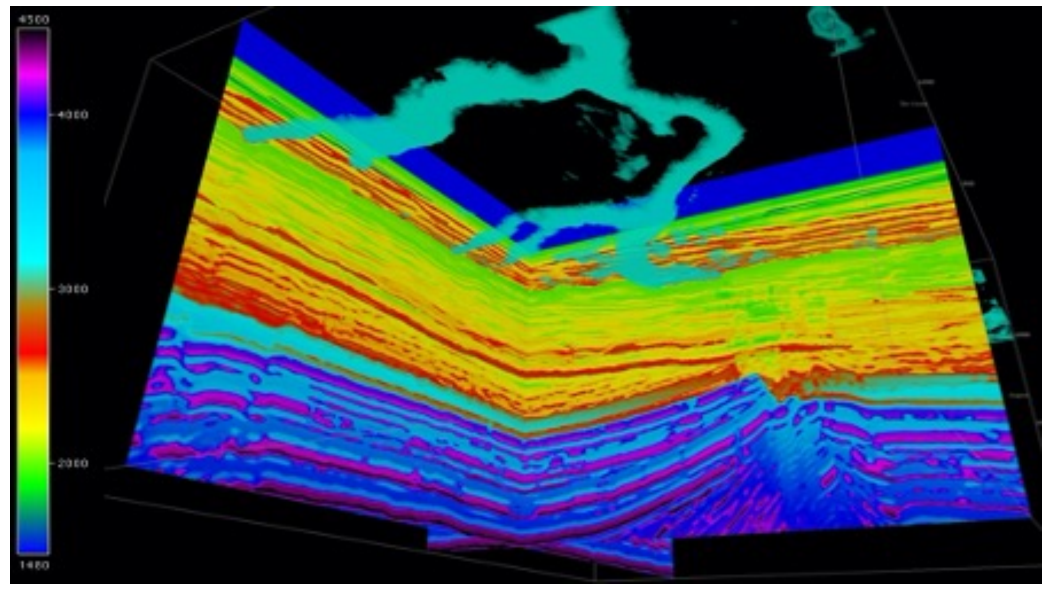

Seismic model
wave speed, density

Build proxy model

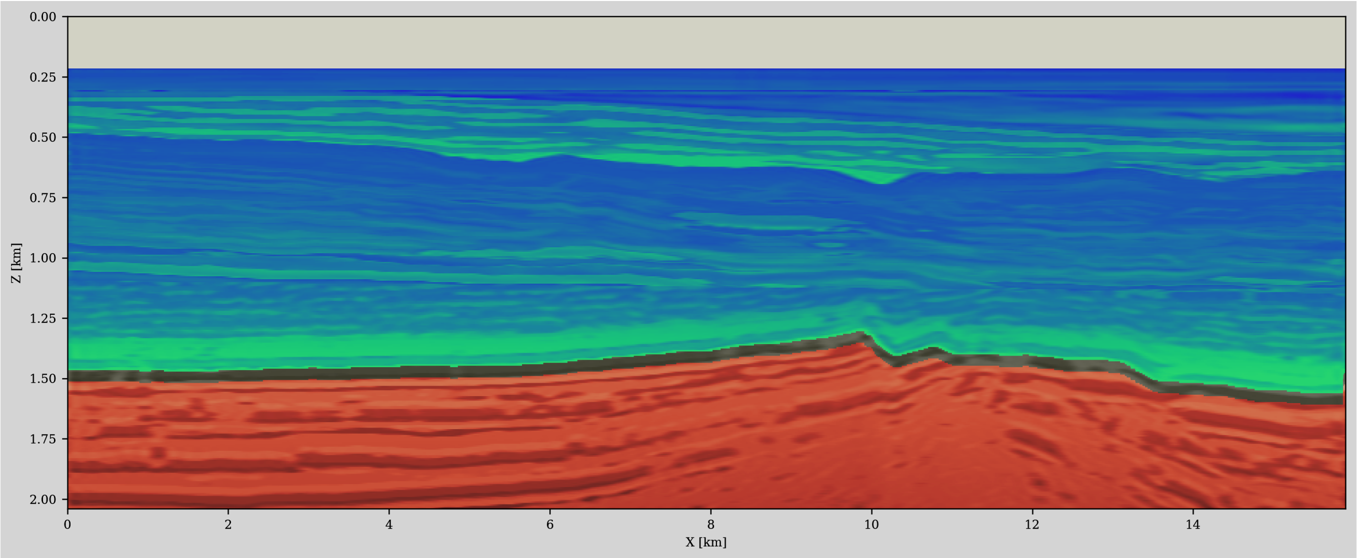

Fluid model
permeability, porosity

Reservoir simulation

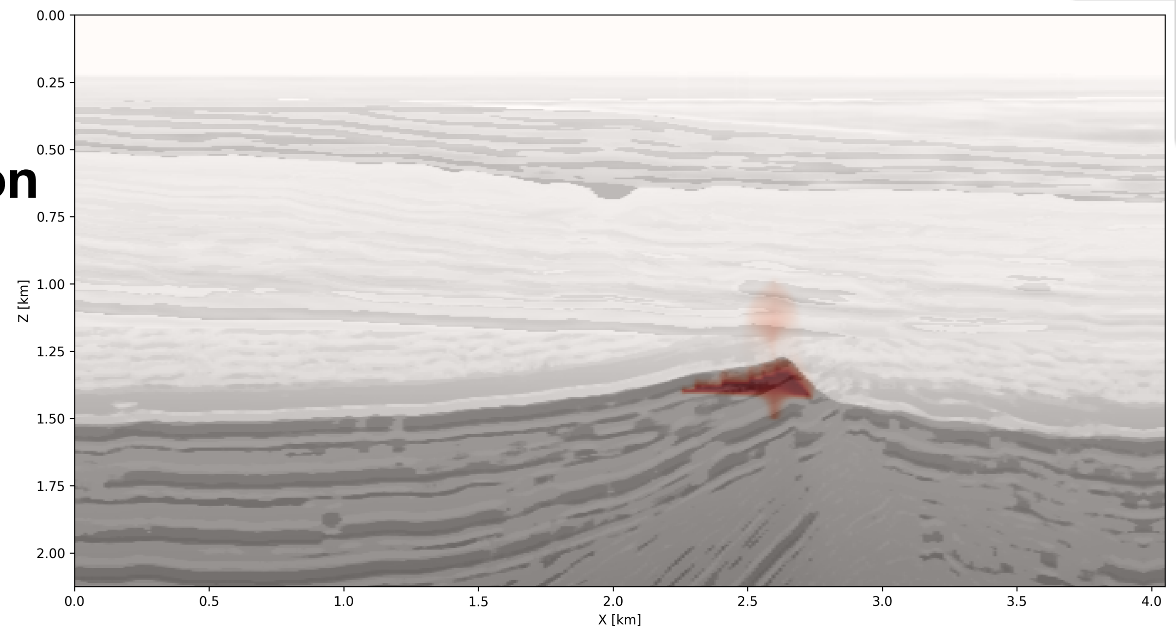

CO_2 dynamics
saturation, pressure

Rock physics

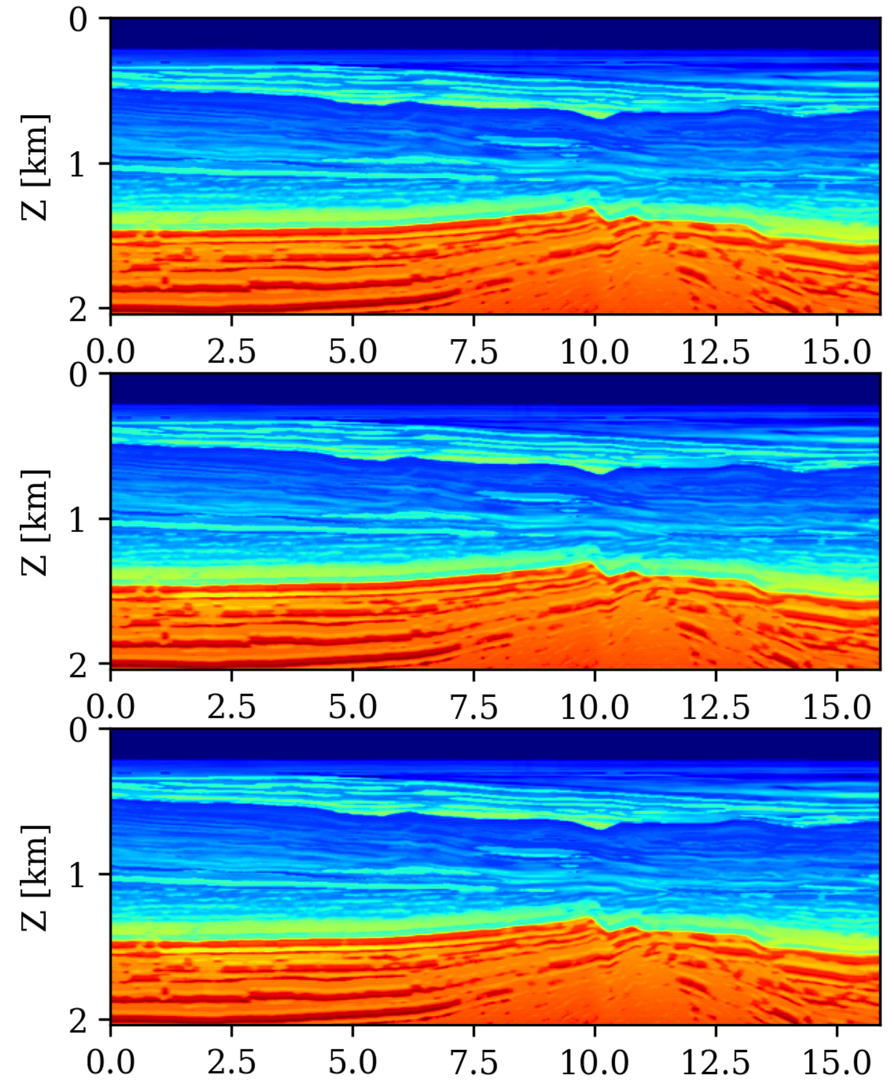

Time-lapse seismic model
wave speed, density

Seismic modeling

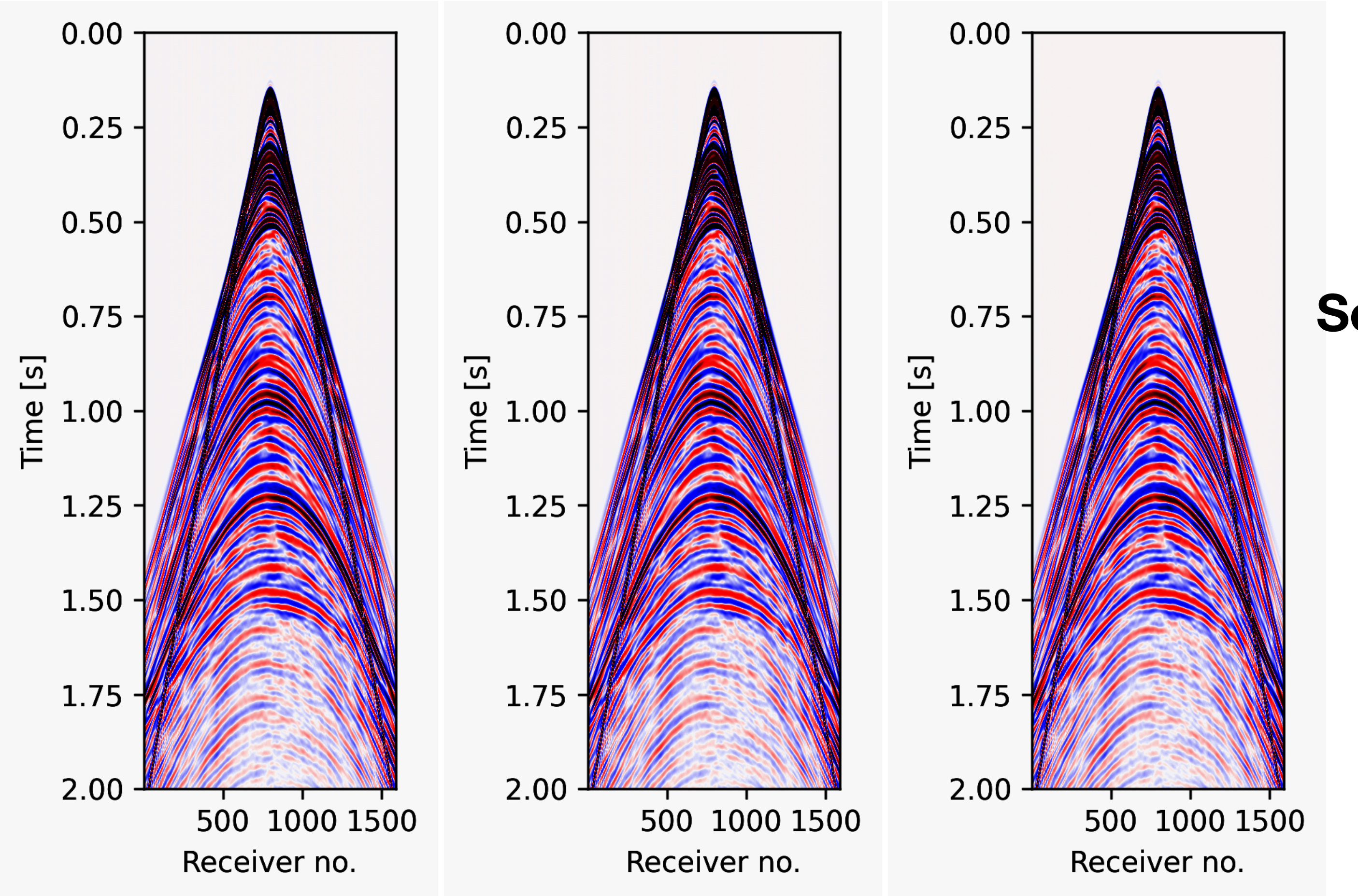

Time-lapse seismic data
pressure

Seismic imaging

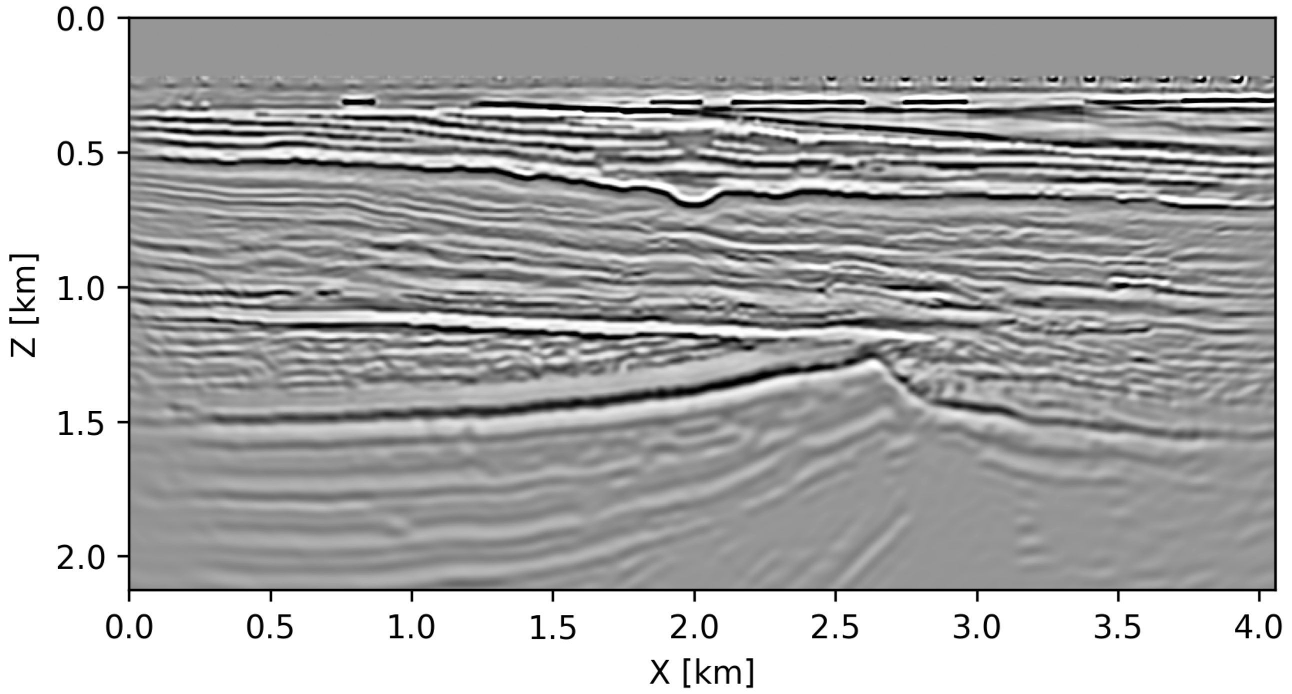

Time-lapse seismic images
impedance contrast

Full-scale proxy models
heterogeneity constrained by 3D seismic & well-data

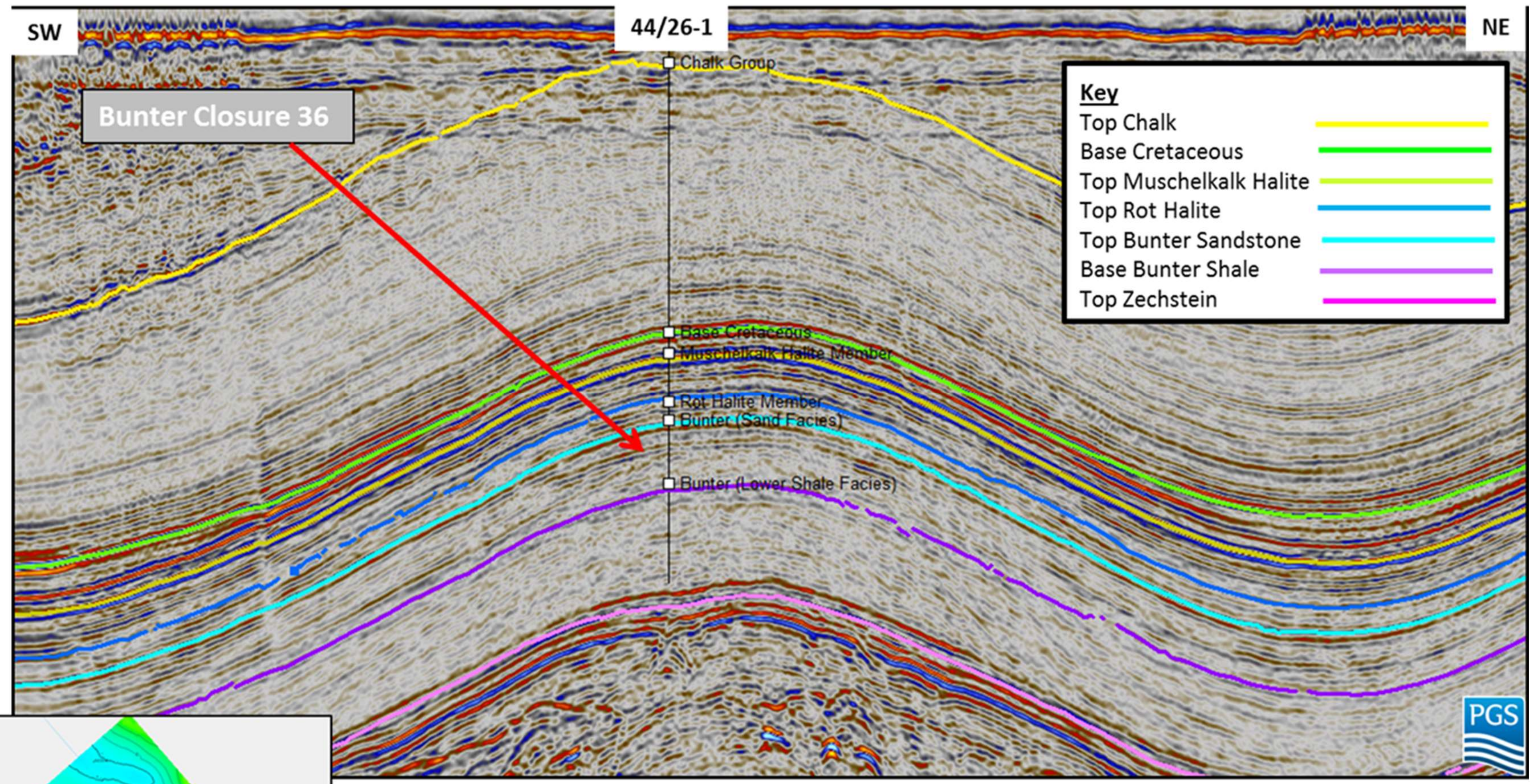

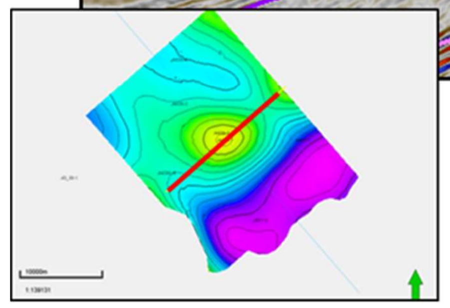

SW-NE seismic line from PGS Megasurvey showing horizons interpreted.

Bunter Closure 36 is highlighted.

from: Strategic UK CCS Storage Appraisal Project

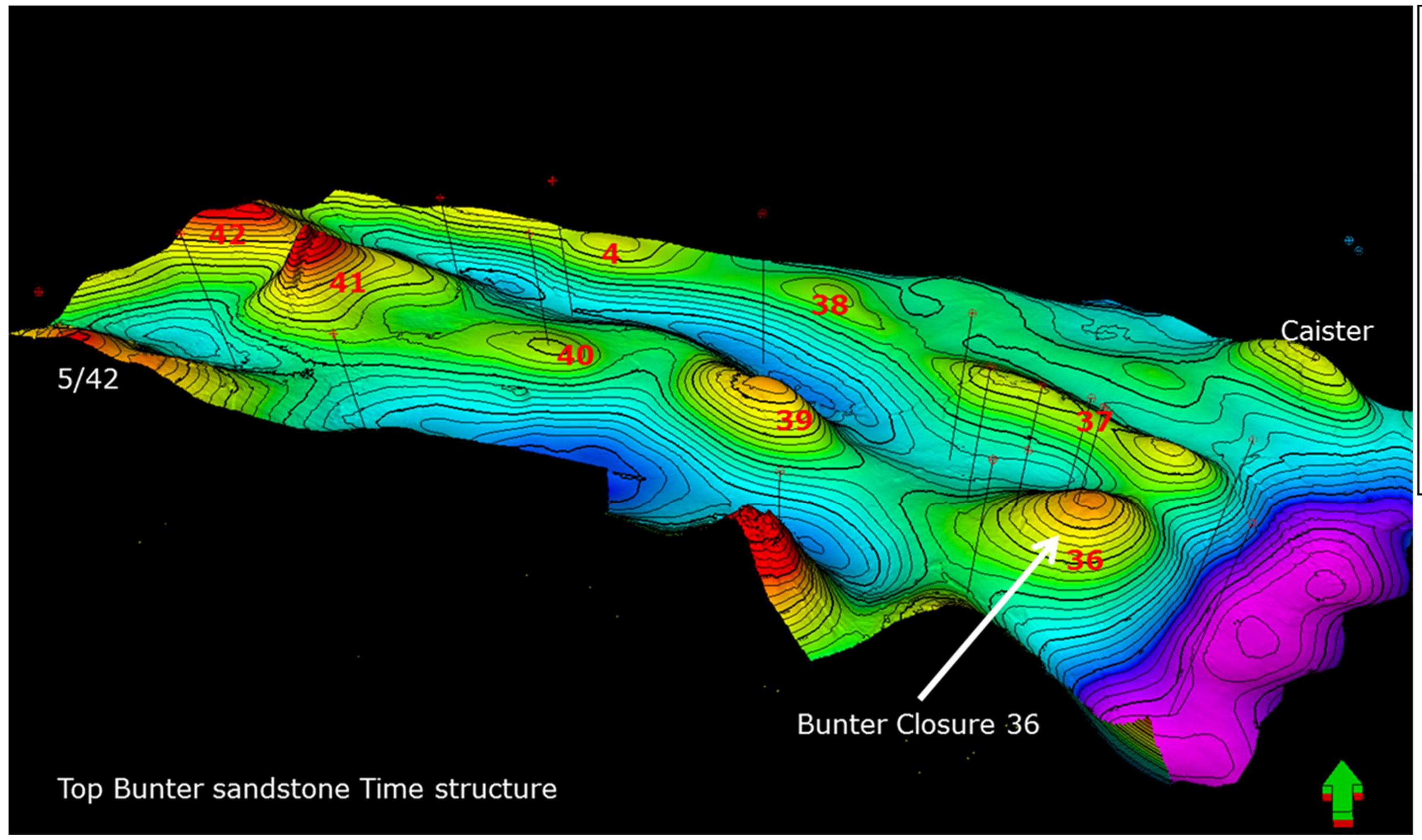

3D view of Top Bunter Sandstone two-way time structure over the Fairway and Closure 36.

Shows 8 anticlines with the UKSAP numbers plus 5/42 and Caister.

Translate 3D post-stack seismic into 3D proxy models for velocity & density

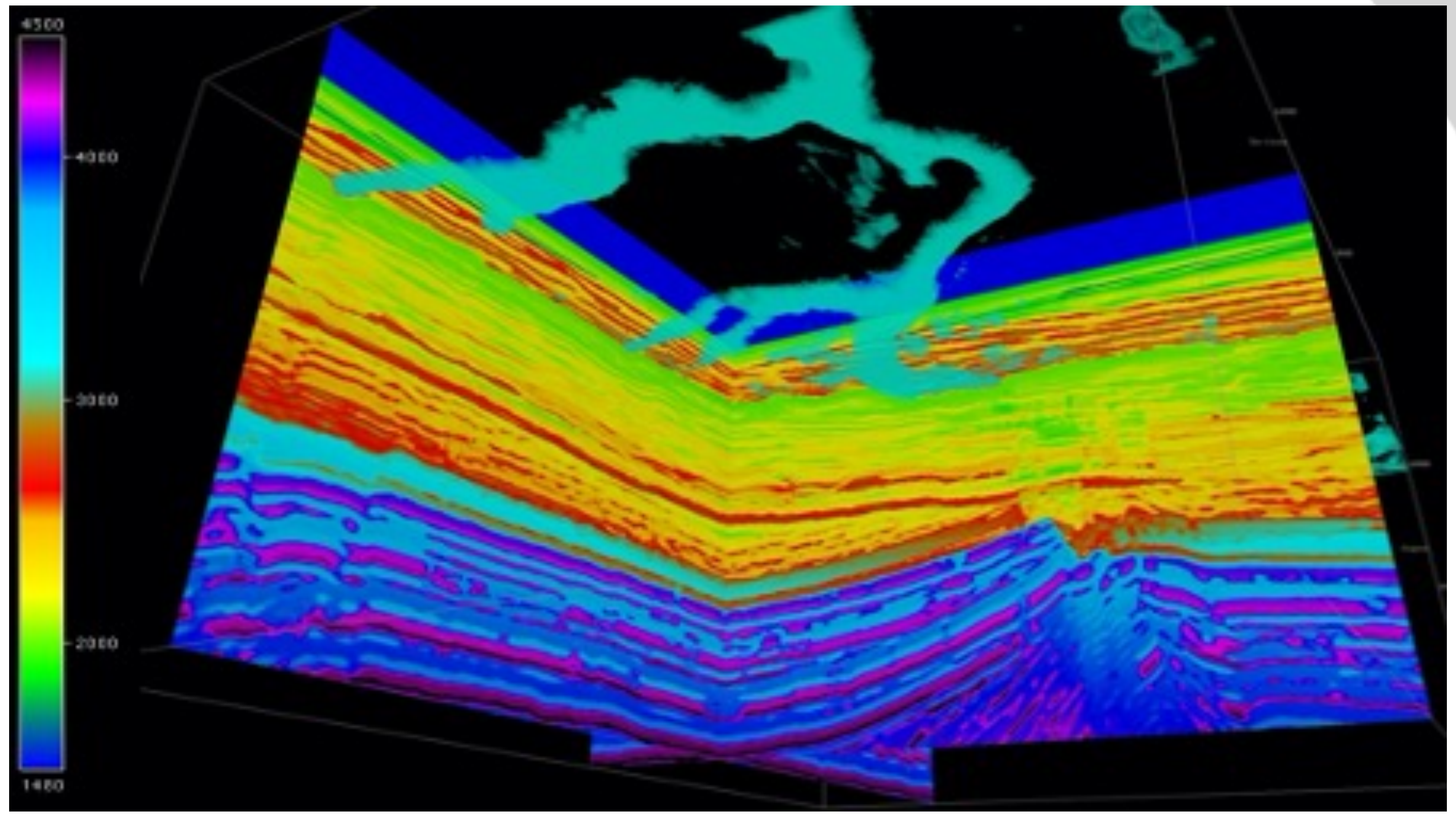

compressional wavespeed

≫15km

Built to test FWI technology

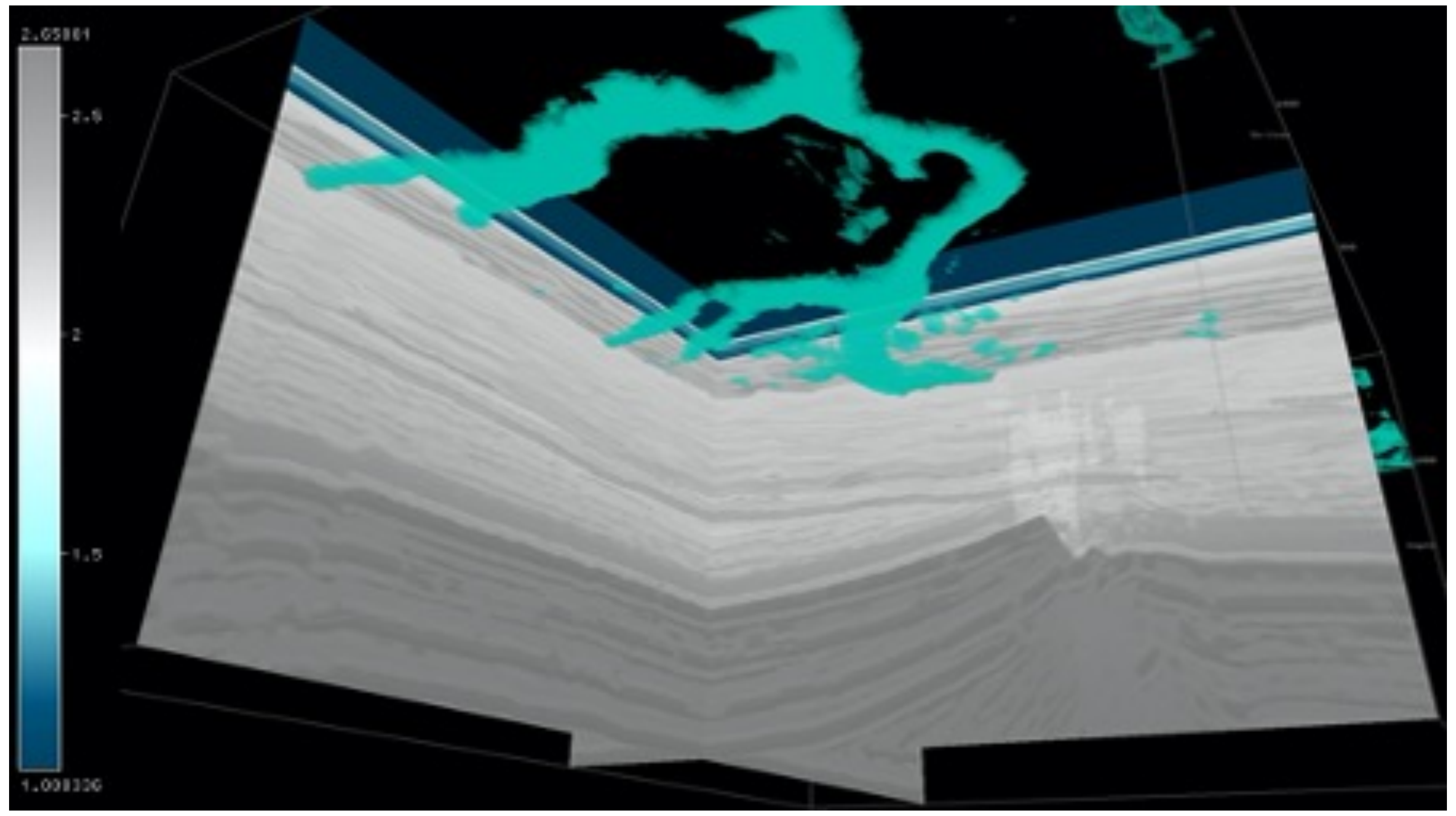

density

Jones, C. E., et al. "Building complex synthetic models to evaluate acquisition geometries and velocity inversion technologies." European Association of Geoscientists & Engineers, 2012.

Conversion

velocity $\Longrightarrow$ permeability

Converted with v_p 1km/s ↑ ⇒ K 1.63mD ↑

- K permeability
- v_p compressional wave speed

Three main geologic sections:

- secondary seal – Haisborough group (blue, $> 300\text{m}$, permeability $15 - 18\text{mD}$)
- primary seal – Rote Halite member (black, 50m, permeability $10^{-4} - 10^{-2}\text{mD}$)
- saline aquifer – Bunter sandstone (red, $300 - 500\text{m}$, permeability $> 170\text{mD}$)

Values taken from Strategic UK CCS Storage Appraisal Project

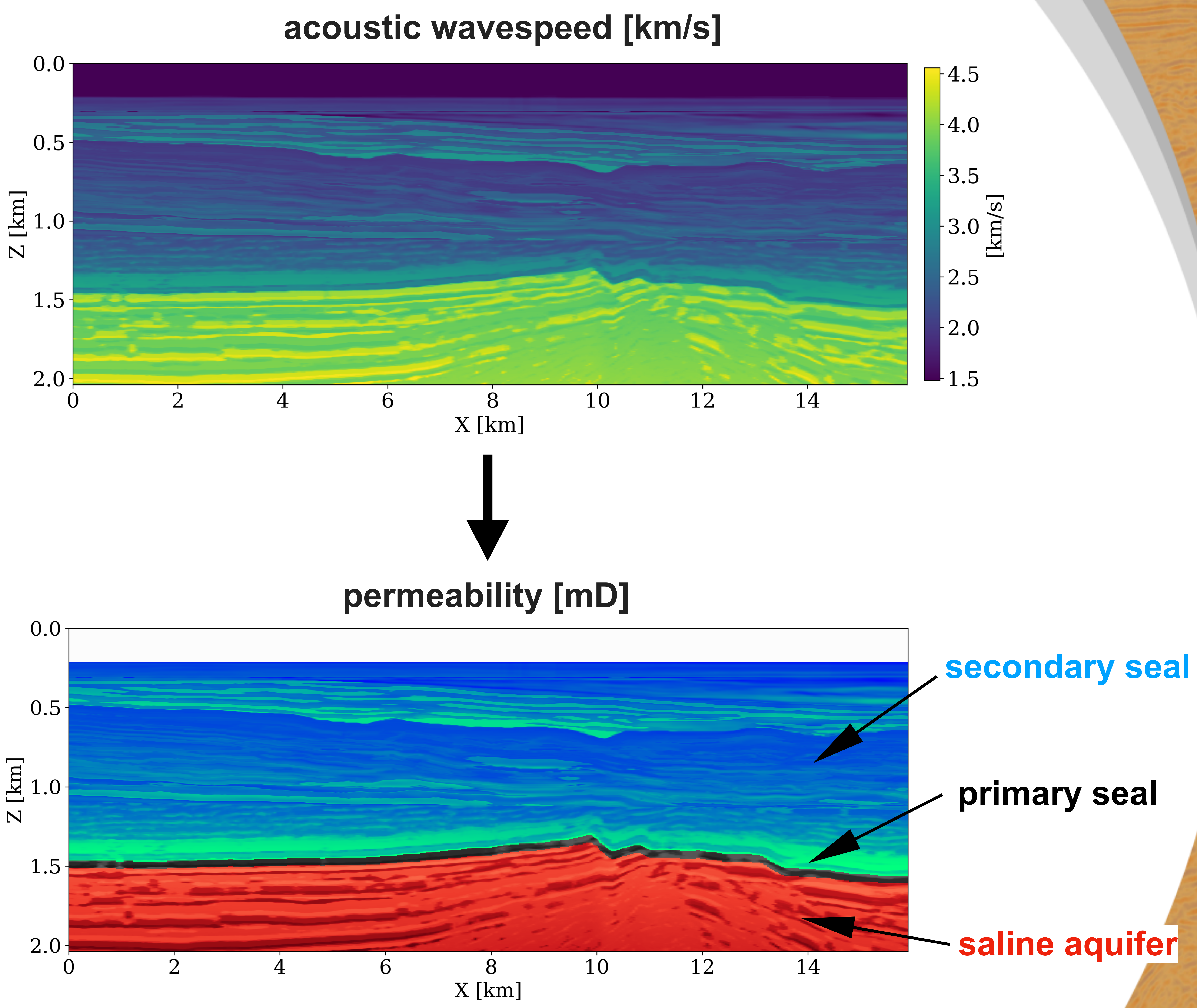

Costa, Antonio. "Permeability-porosity relationship: A reexamination of the Kozeny-Carman equation based on a fractal pore-space geometry assumption." Geophysical research letters 33.2 (2006).

Conversion

permeability $\Longrightarrow$ porosity

Kozeny-Carman relationship:

$$K = \phi^3 \left(\frac{1.527}{0.0314 * (1 - \phi)} \right)^2$$

- K permeability
- ϕ porosity
- values taken from Strategic UK CCS Storage Appraisal Project

Permeability & porosity models serve as input for two-phase fluid flow simulations.

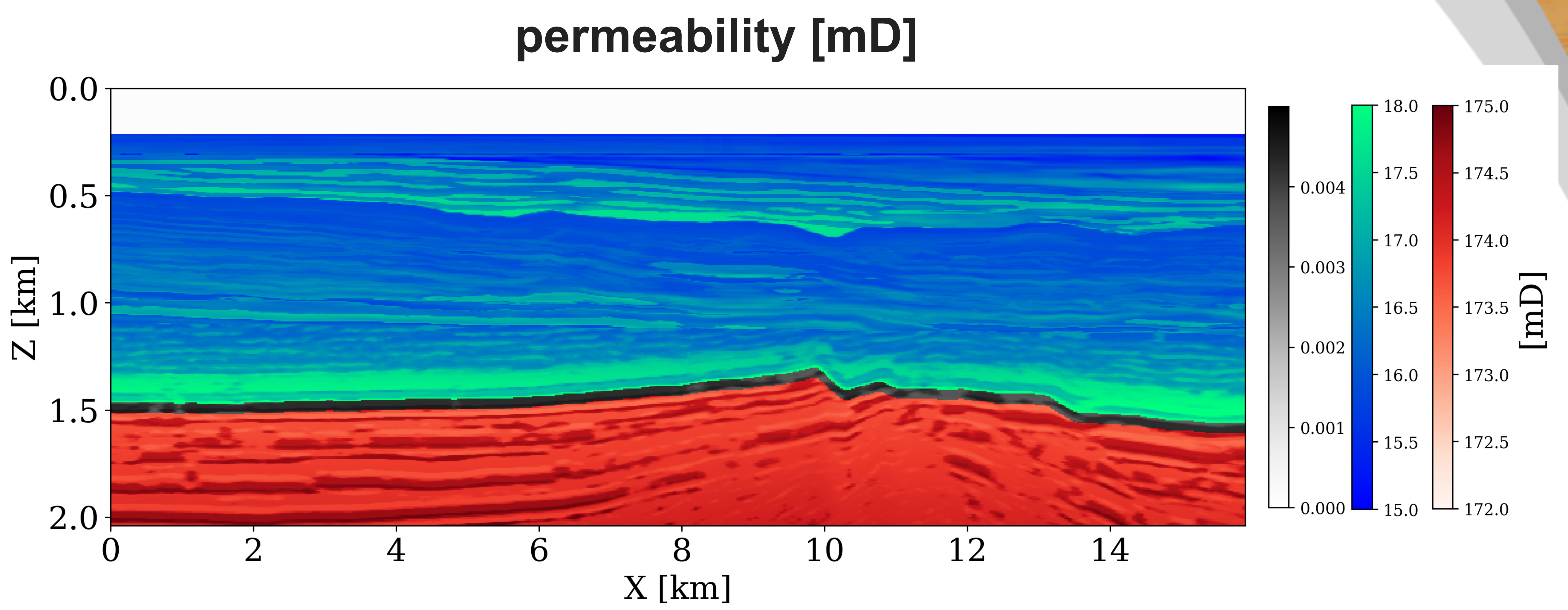

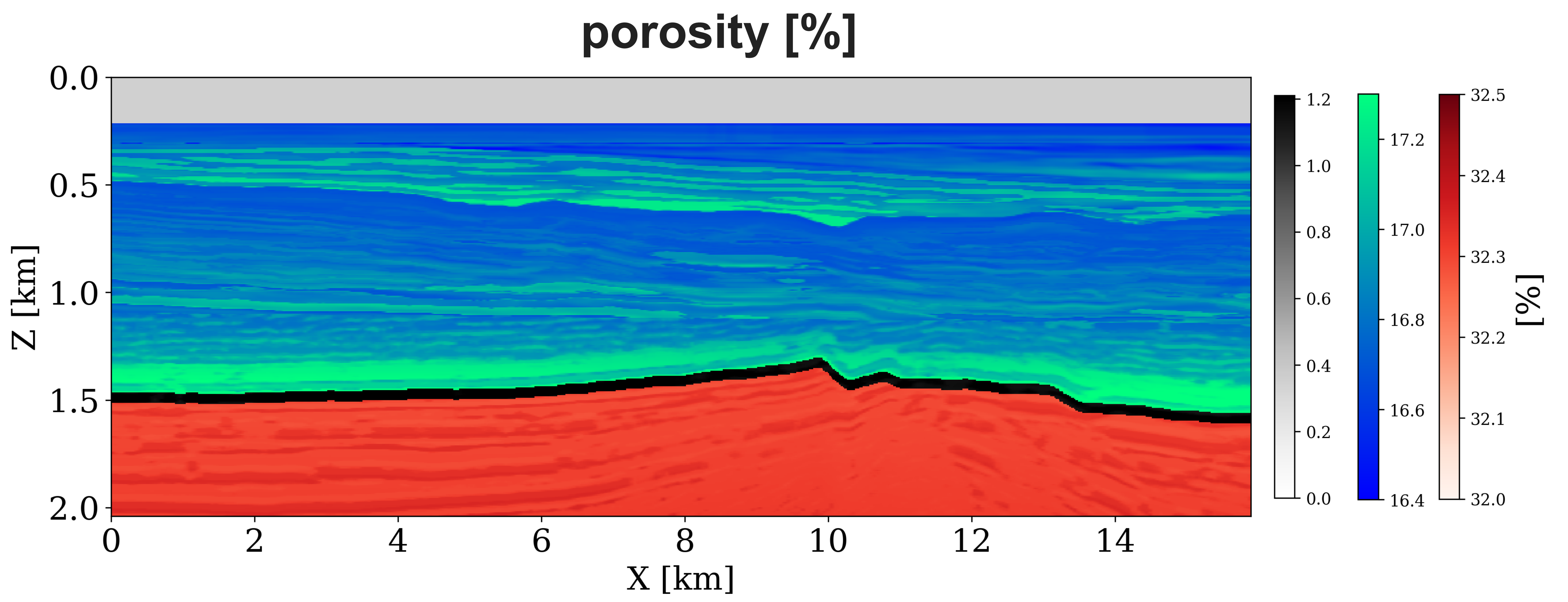

CO_2 injection
Compass proxy model

Synthetic 100-year CCS project in the North Sea

- inject 7Mt/y of CO_2 for 60 years
- monitor by active-source seismic imaging
- 5 seismic surveys: baseline & 15, 30, 45, 60 years after injection

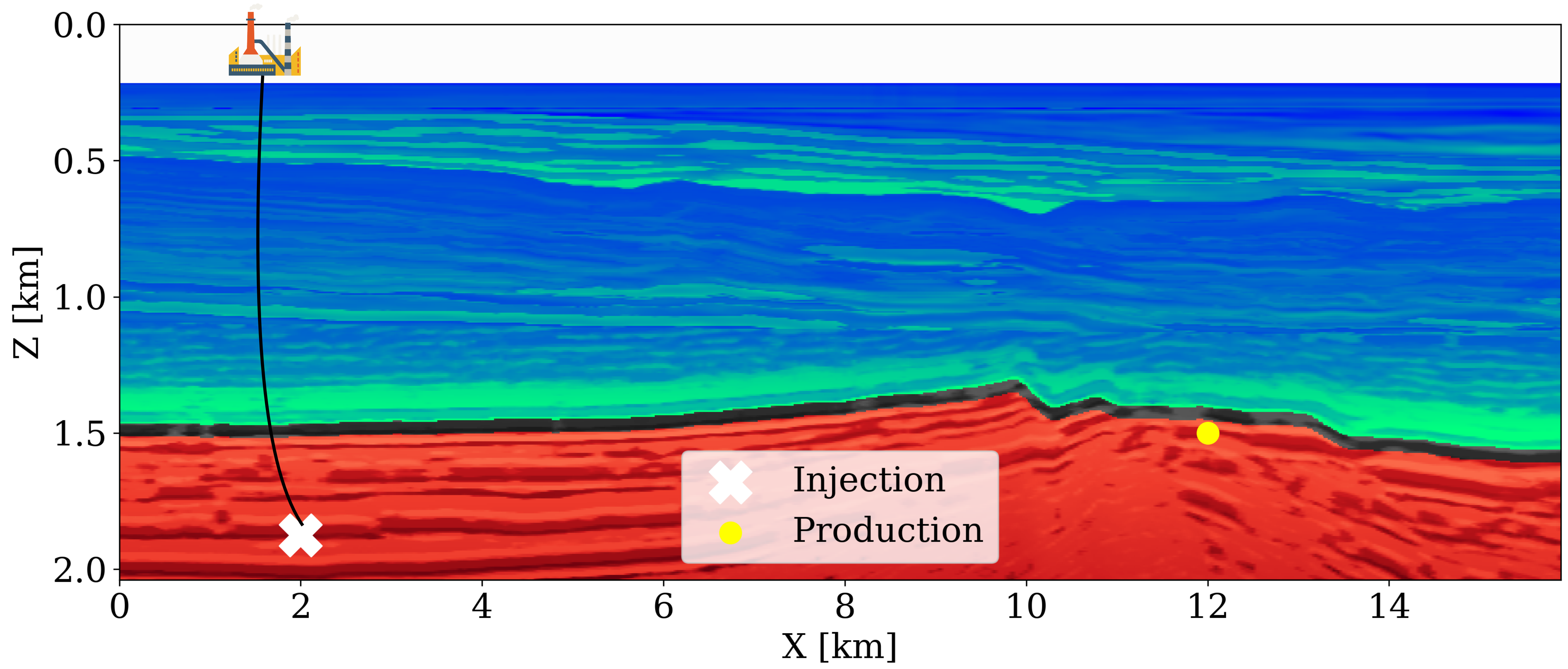

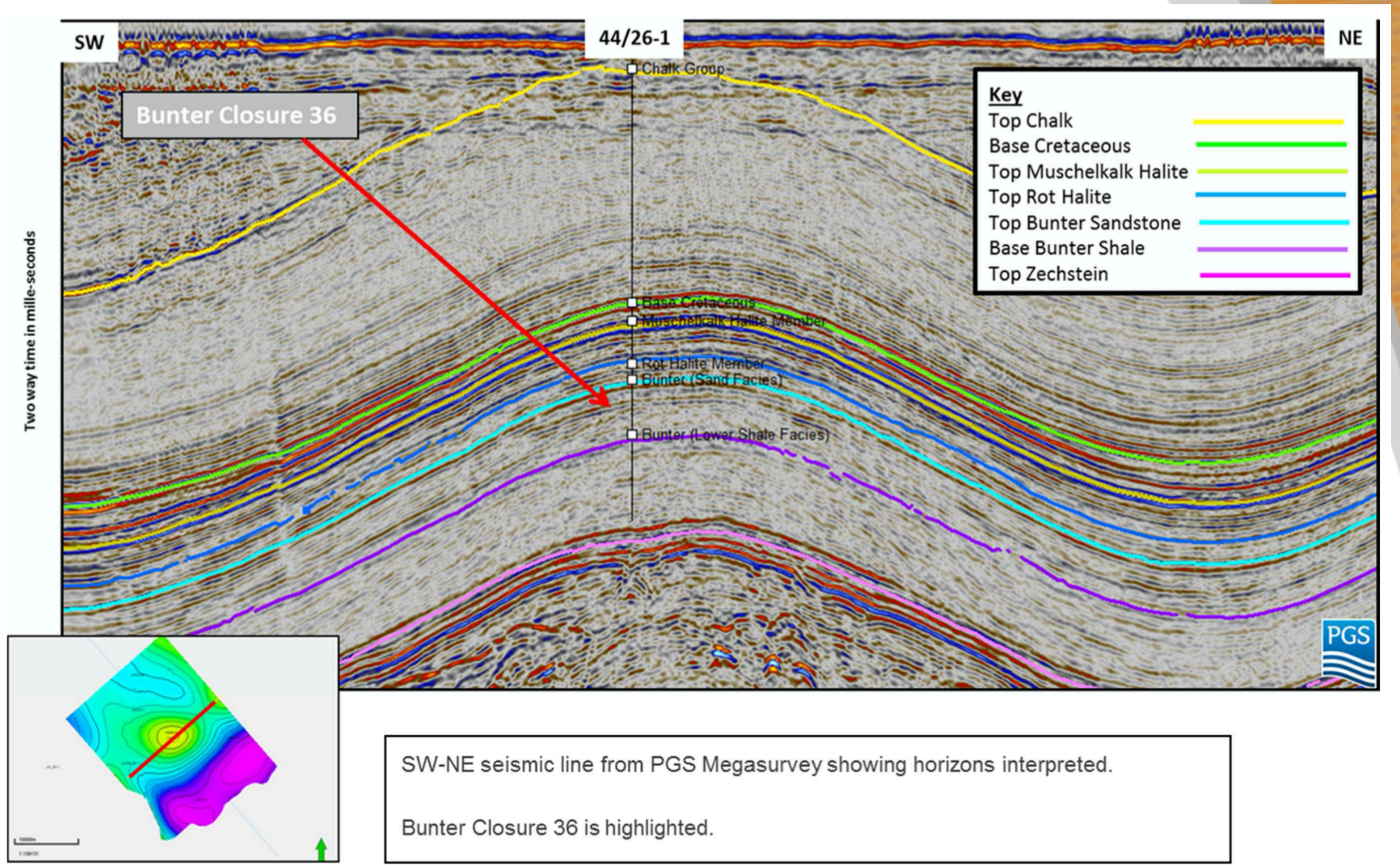

Strategic UK CCS Storage Appraisal Project

Li, Dongzhuo, et al. "Coupled Time-Lapse Full-Waveform Inversion for Subsurface Flow Problems Using Intrusive Automatic Differentiation." Water Resources Research 56.8 (2020): e2019WR027032.

CO_2 dynamics

two-phase flow equations

mass balance equation:

$$\frac{\partial}{\partial t}(\phi S_i \rho_i) + \nabla \cdot (\rho_i \mathbf{v}_i) = \rho_i q_i, \quad i = 1,2$$

inject CO_2 to replace water

$$S_1 + S_2 = 1$$

Darcy's law:

$$\mathbf{v}_i = -\frac{K k_{ri}}{\tilde{\mu}_i}(\nabla P_i - g \rho_i \nabla Z), \quad i = 1,2$$

Corey model:

$$k_{ri}(S_i) = S_i^2$$

fluid pressure:

$$P_2 = P_1 - P_c(S_2)$$

Symbol	Meaning
K	permeability
ϕ	porosity
k_{ri}	relative permeability
S_i	fluid saturation
P_i	fluid pressure
P_c	capillary pressure
$\mathbf{v}_i$	Darcy's velocity
ρ_i	fluid density
$\tilde{\mu}_i$	fluid viscosity
q_i	injection/production rate
g	gravity constant
Z	vector of vertical direction

CO_2 dynamics

two-phase flow simulation

grid spacing 25m, time step 20 days

stop injection at 60th year

model extends 1.6km in perpendicular direction

CO_2 movement driven by buoyancy

420 Mt CO_2 injected during CCS project

CO_2 concentration [%] for every 5 years

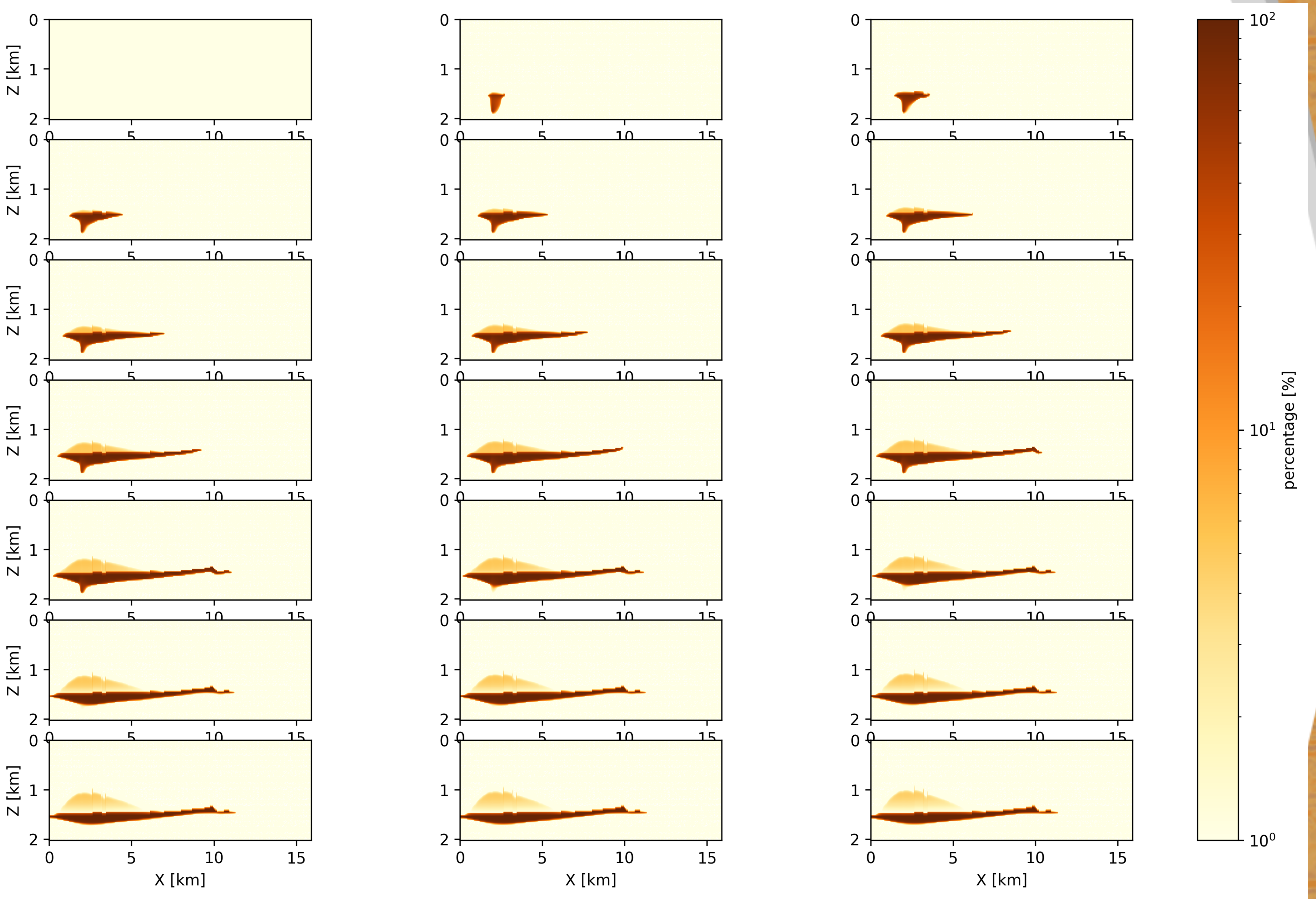

CO_2 saturation
baseline

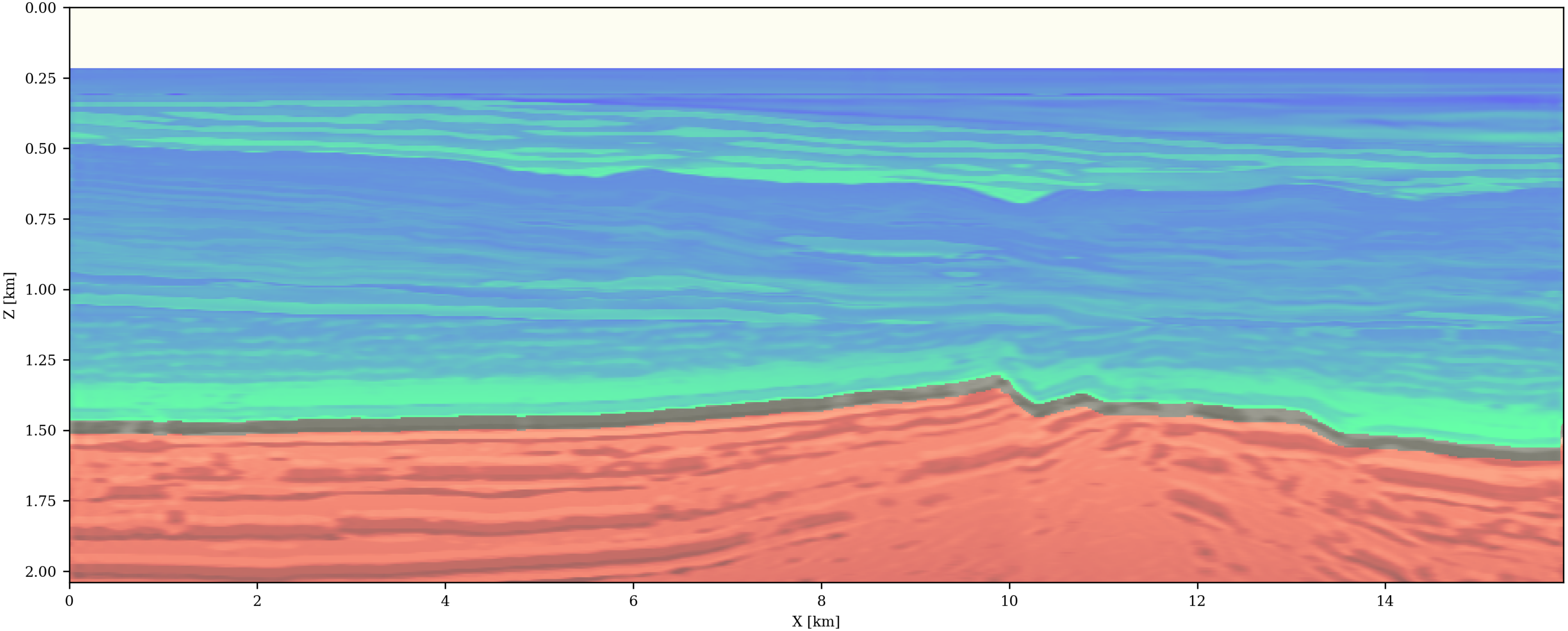

CO_2 saturation
monitor 1 — 15 years after injection

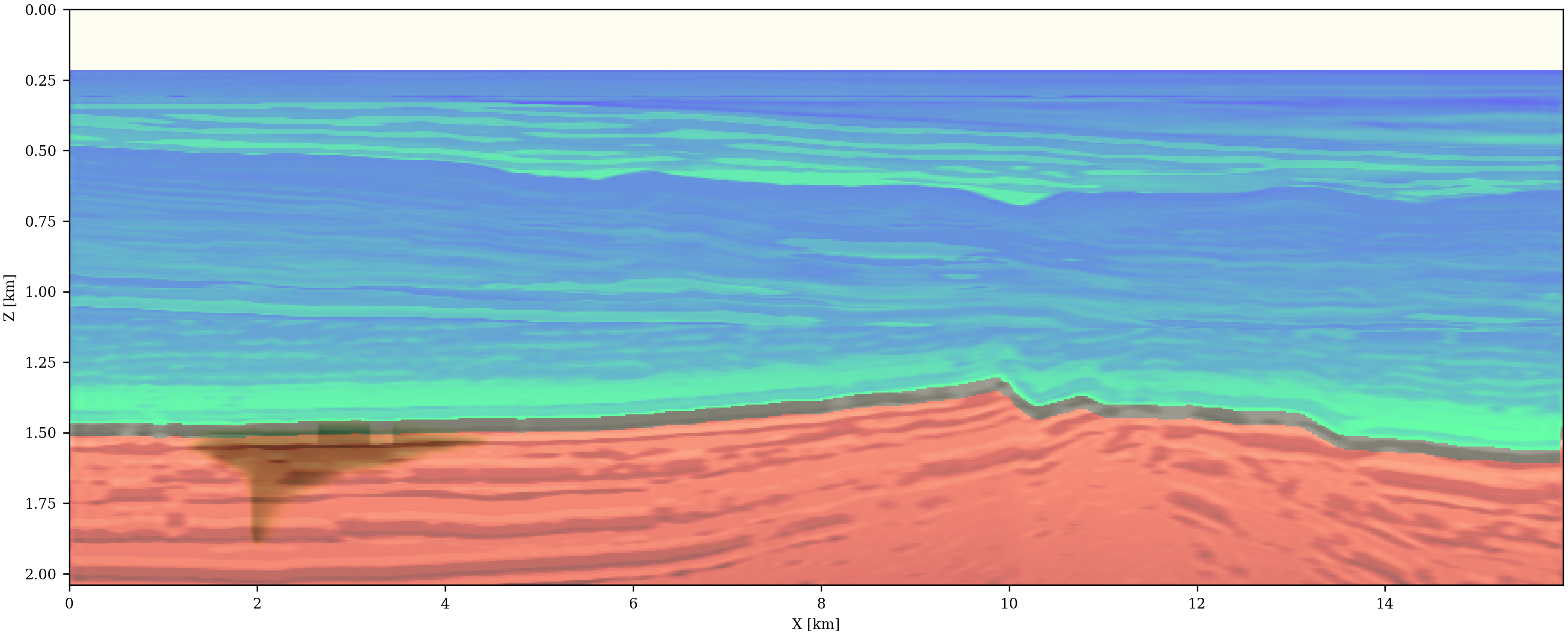

CO_2 saturation
monitor 2 — 30 years after injection

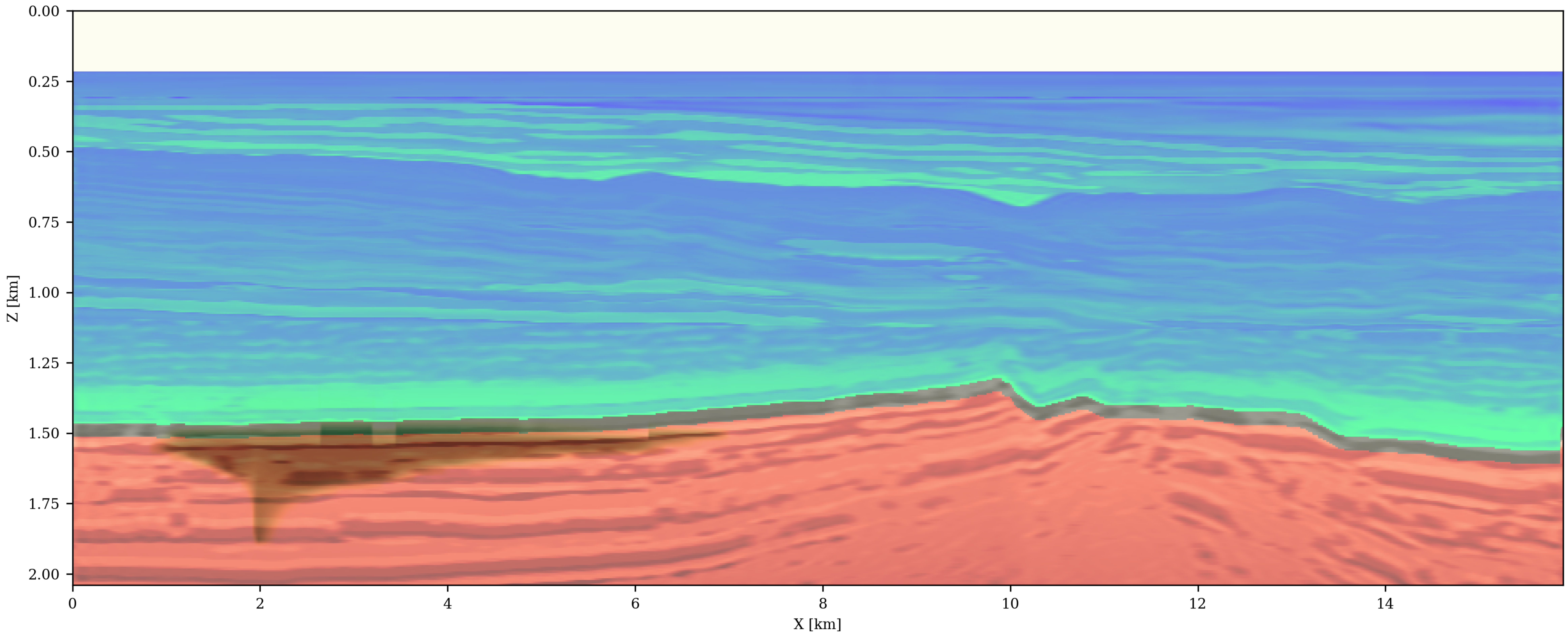

CO_2 saturation
monitor 3 — 45 years after injection

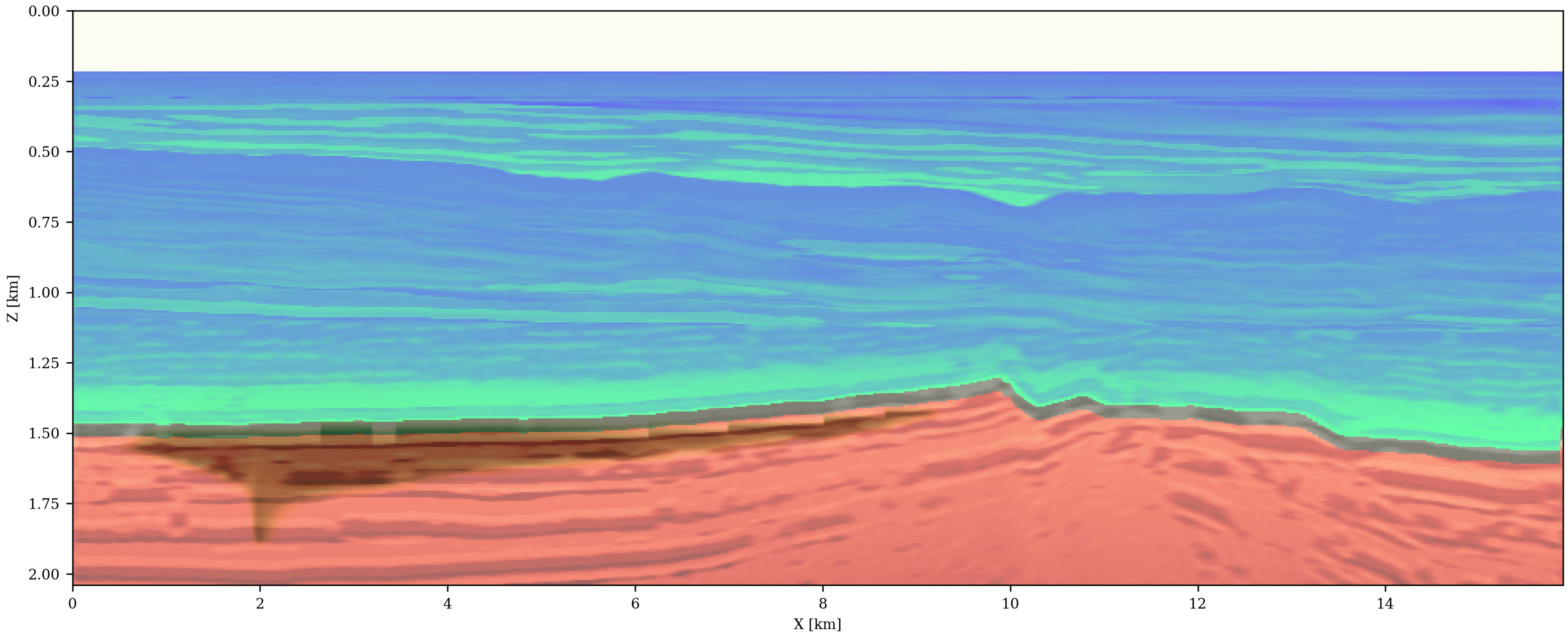

CO_2 saturation

monitor 4 — 60 years after injection

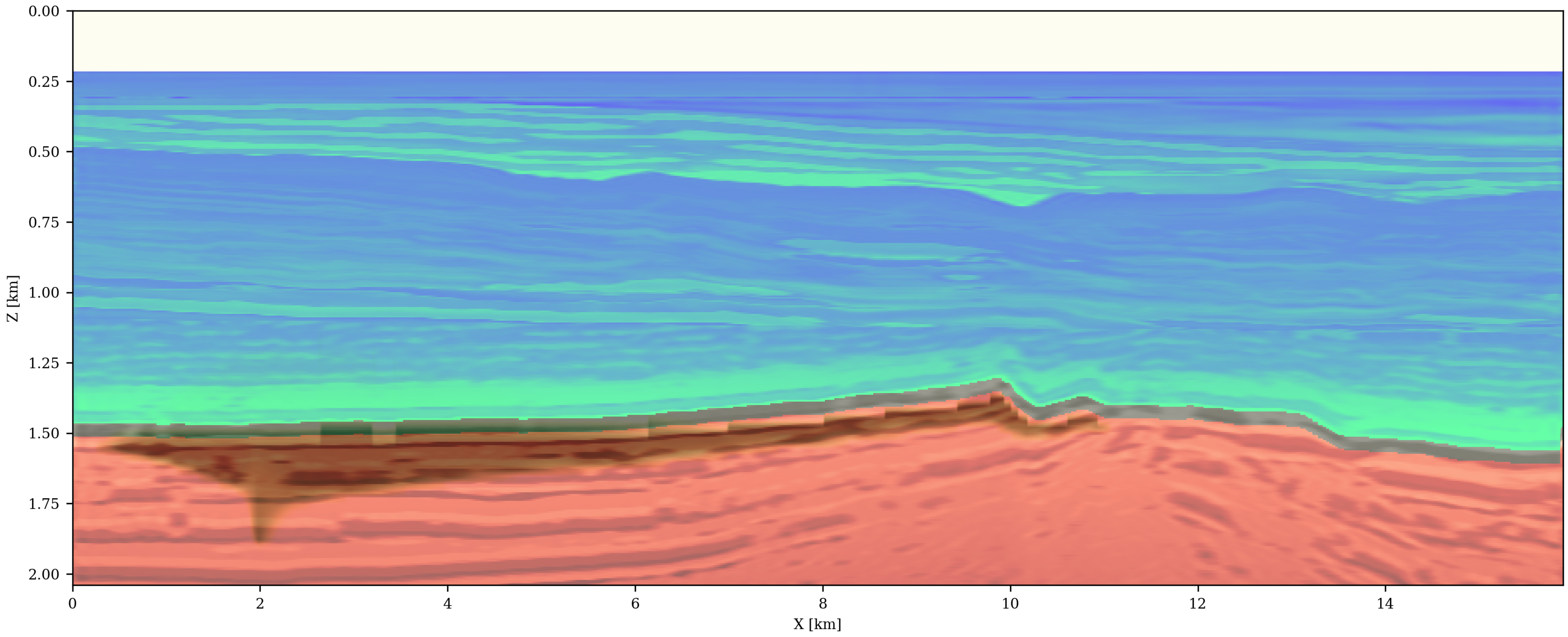

Rock physics
Patchy saturation model

δv_p **velocity changes**

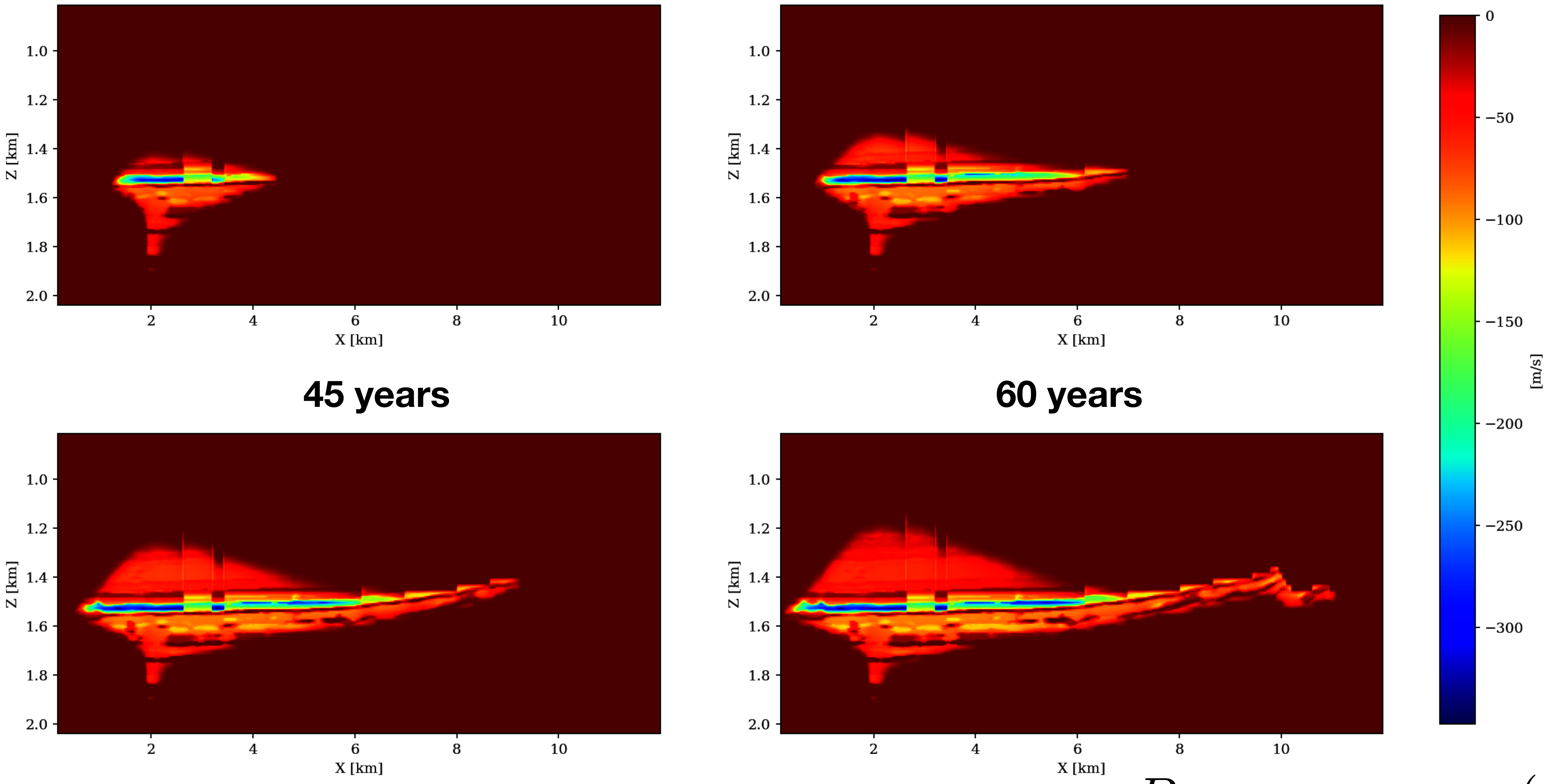

Symbol	Meaning
B_{r1}/B_{r2}	bulk modulus of rock fully saturated with fluid 1/2
B_{f1}/B_{f2}	fluid bulk modulus
ρ_{f1}/ρ_{f2}	fluid density
μ_r	rock shear modulus
v_p/v_s	rock P/S-wave velocity
B_o	bulk modulus of rock grains
ρ_r	rock density
ϕ	rock porosity
S	CO_2 saturation

- CO_2 concentration $\uparrow \longrightarrow v_p \downarrow$
- Decrease by 0-300 m/s
- Localized time-lapse changes
- v_p after 15, 30, 45, 60 years of injection

$$
\begin{aligned}
B_{r1} &= \rho_r(v_p^2 - \tfrac{4}{3}v_s^2) \\
\mu_r &= \rho_r v_s^2 \\
\frac{B_{r2}}{B_o - B_{r2}} &= \frac{B_{r1}}{B_o - B_{r1}} - \frac{B_{f1}}{\phi(B_o - B_{f1})} + \frac{B_{f2}}{\phi(B_o - B_{f2})} \\
\hat{B}_r &= [(1-S)(B_{r1} + \tfrac{4}{3}\mu_r)^{-1} + S(B_{r2} + \tfrac{4}{3}\mu_r)^{-1}]^{-1} - \tfrac{4}{3}\mu_r \\
\hat{\rho}_r &= \rho_r + \phi S(\rho_{f2} - \rho_{f1}) \\
\hat{v}_p &= \sqrt{\frac{\hat{B}_r + \frac{4}{3}\mu_r}{\hat{\rho}_r}}
\end{aligned}
$$

Per Avseth, et al. Quantitative seismic interpretation: Applying rock physics tools to reduce interpretation risk. Cambridge university press, 2010.

Idealized acquisition
replicated dense surveys

Louboutin, Mathias, et al. "Devito (v3. 1.0): an embedded domain-specific language for finite differences and geophysical exploration." *Geoscientific Model Development* 12.3 (2019): 1165-1187.
Luporini, Fabio, et al. "Architecture and performance of Devito, a system for automated stencil computation." *ACM Transactions on Mathematical Software (TOMS)* 46.1 (2020): 1-28.
Witte, Philipp A., et al. "A large-scale framework for symbolic implementations of seismic inversion algorithms in Julia." *Geophysics* 84.3 (2019): F57-F71.

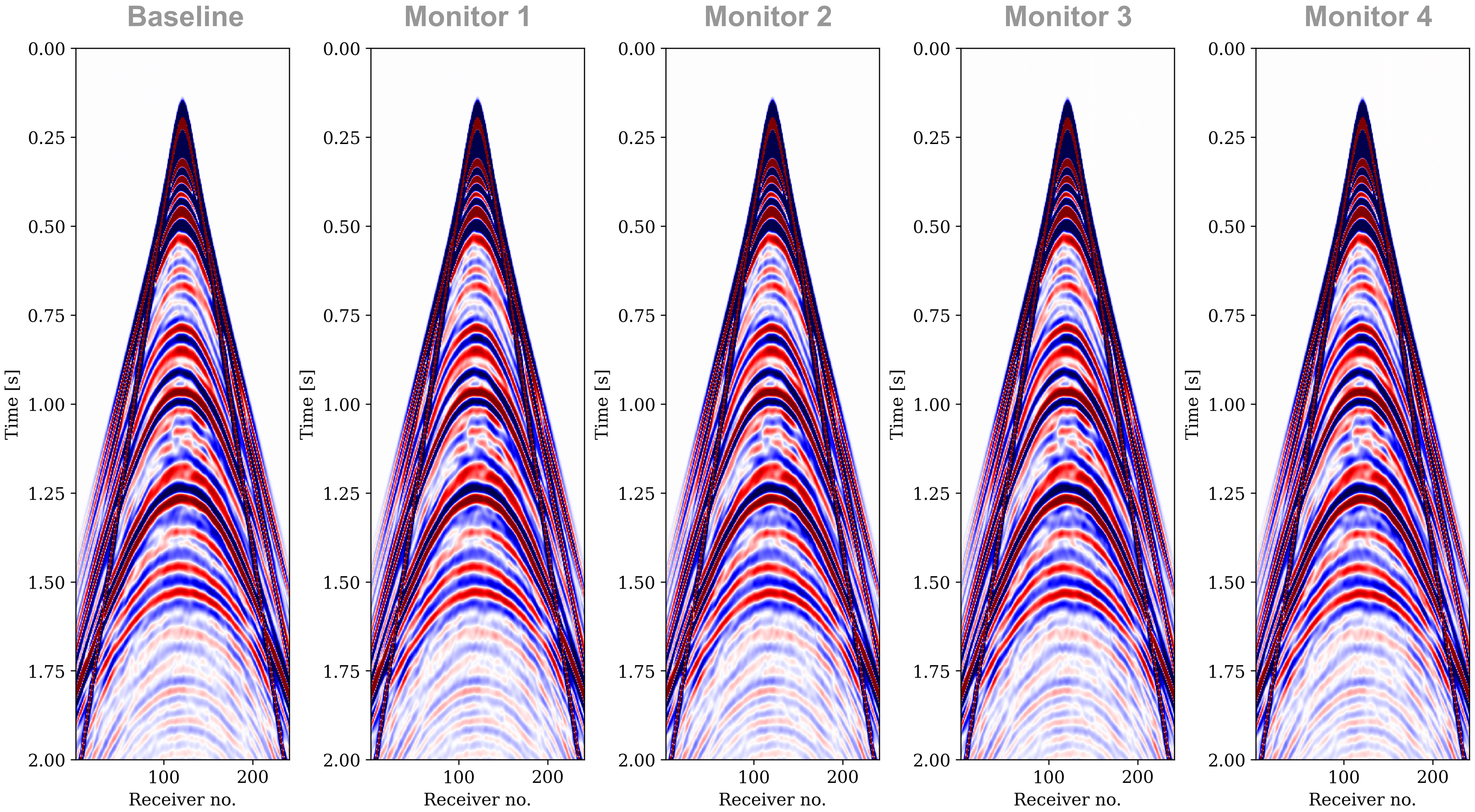

Ideal time-lapse signal

5 X direct subtraction

Time-lapse signal is very weak

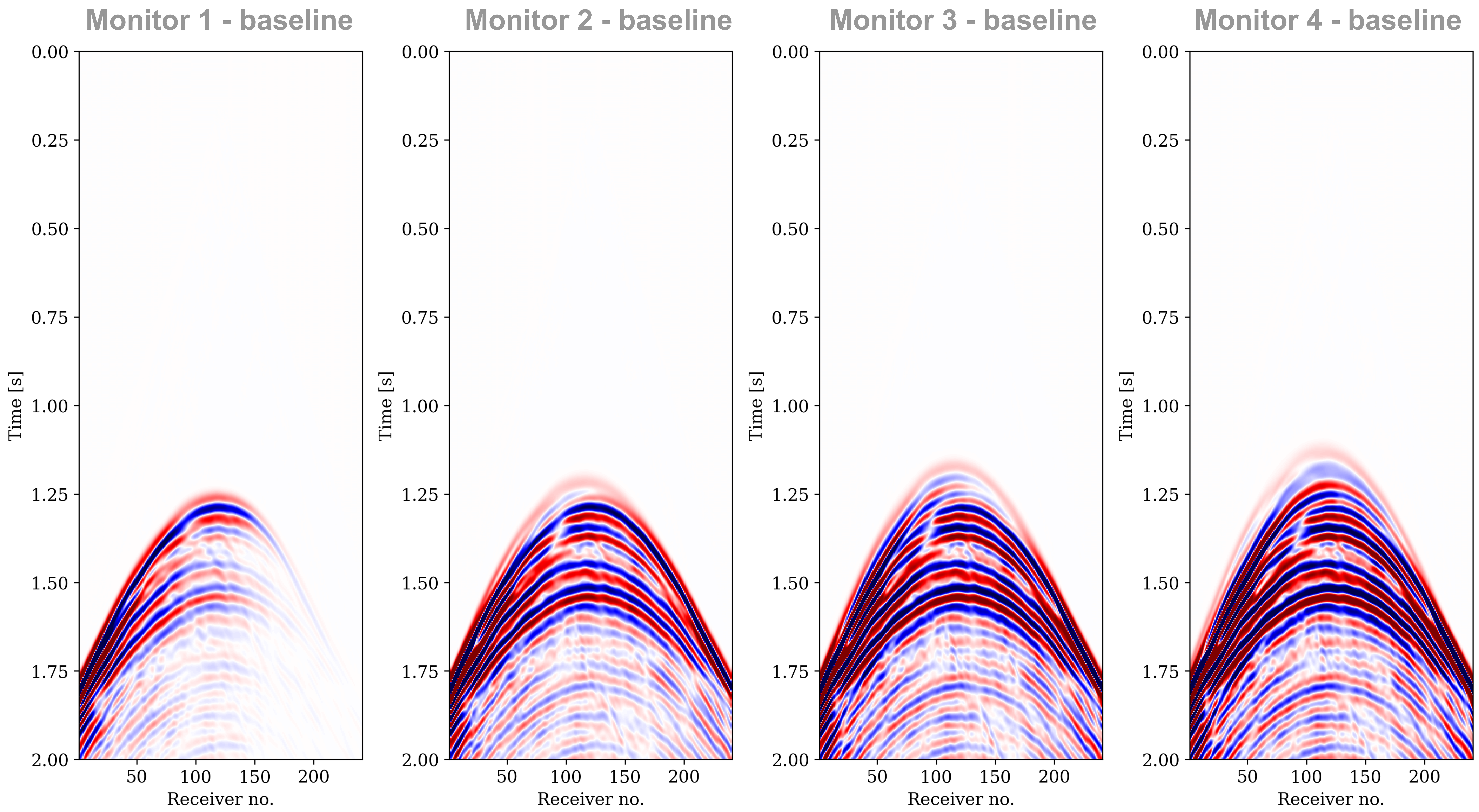

Realistic time-lapse signal
subtraction after binning data w/ non-replicated source locations

Time-lapse signal corrupted by binning from non-replicated acquisition

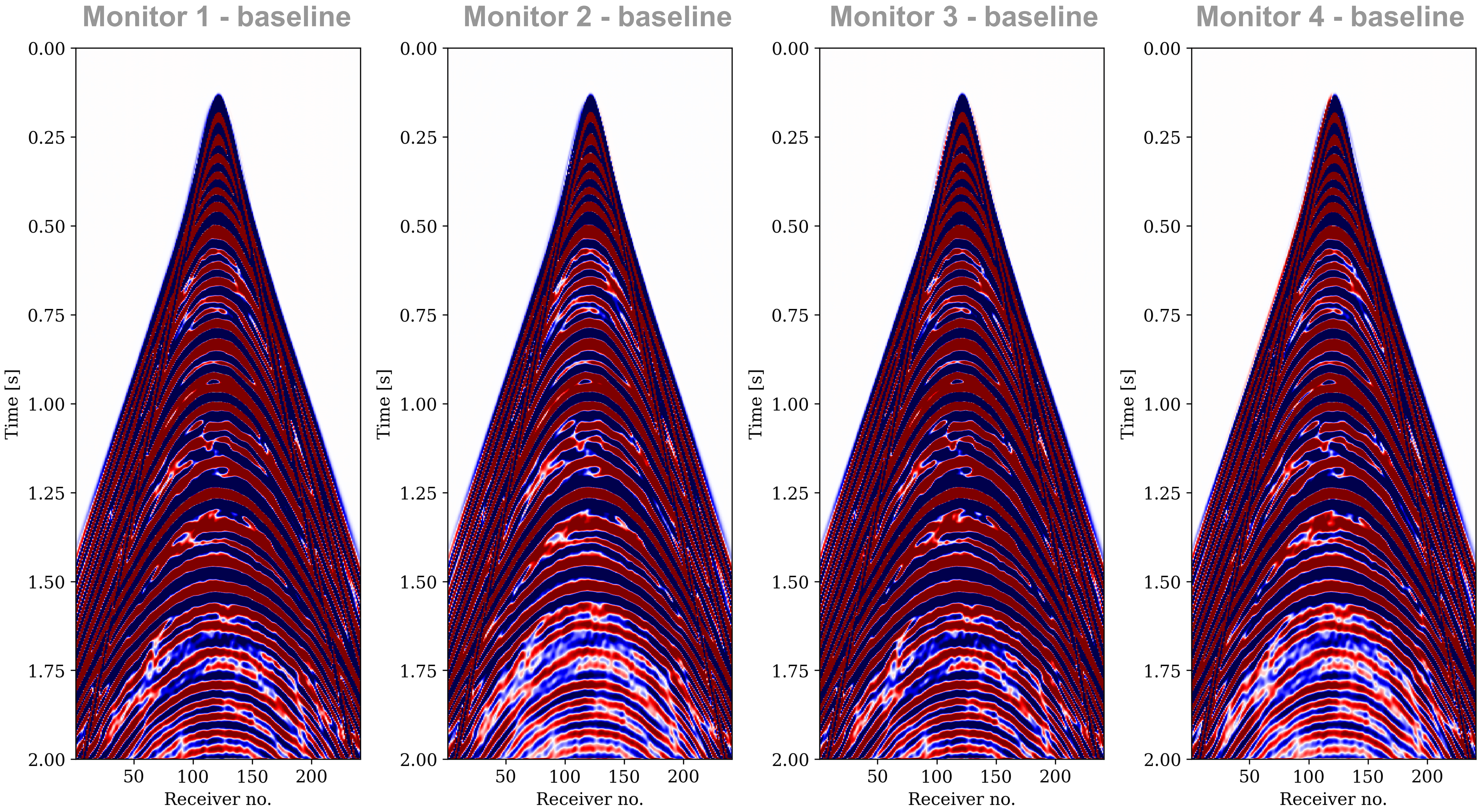

Zhou, Wei, and David Lumley. "Central-difference time-lapse 4D seismic full-waveform inversion." *Geophysics* 86.2 (2021): R161-R172.
Oghenekohwo, F., Wason, H., Esser, E., and Herrmann, F. J., 2017, Low-cost time-lapse seismic with distributed compressive sensing-part 1: Exploiting common information among the vintages: Geophysics
Wason, H., Oghenekohwo, F., and Herrmann, F. J., 2017, Low-cost time-lapse seismic with distributed compressive sensing-part 2: Impact on repeatability: Geophysics
Wei, L., Tian, Y., Li, C., Oppert, S., and Hennenfent, G., 2018, Improve 4D seismic interpretability with joint sparsity recovery: In SEG technical program expanded abstracts 2018 (pp. 5338–5342). Society of Exploration Geophysicists.

SLIM

Practical challenges

time-lapse seismic monitoring of CCS

Seismic monitoring of CCS is challenging because

- seismic acquisitions NOT replicated amongst different surveys
- amplitude of time-lapse signal is very low
- noise corrupts the time-lapse signal

Existing approaches

- double & central differences
- low-cost time-lapse data acquisition & imaging w/ joint recovery model
- joint sparsity recovery for denoising

Seismic Imaging

least-squares reverse-time migration

Linearized modeling $\delta \mathbf{d}_j = \nabla \mathscr{F}_j(\overline{\mathbf{m}}_j)\delta \mathbf{m}_j$ **for** $j = \{1, 2, \cdots, n_v\}$

LS-RTM $\underset{\delta \mathbf{m}_j}{\text{minimize}} \quad \|\delta \mathbf{d}_j - \nabla \mathscr{F}_j(\overline{\mathbf{m}}_j)\delta \mathbf{m}_j\|_2^2$

$\nabla \mathscr{F}_j(\overline{\mathbf{m}}_j)$	linearized forward modeling operator
$\delta \mathbf{d}_j$	linearized data
$\overline{\mathbf{m}}_j$	background model (different for each survey)
$\delta \mathbf{m}_j$	model parameter perturbation
n_v	number of surveys

Lorenz, Dirk A., et al. "A sparse Kaczmarz solver and a linearized Bregman method for online compressed sensing." 2014 IEEE international conference on image processing (ICIP). IEEE, 2014.
Witte, Philipp A., et al. "Compressive least-squares migration with on-the-fly Fourier transforms." Geophysics 84.5 (2019): R655-R672.

Linearized Bregman

sparsity-promoting least-squares migration

For each survey, solve

$$\min_{\mathbf{x}} \quad \lambda\|\mathbf{C}\delta\mathbf{m}\|_1 + \frac{1}{2}\|\mathbf{C}\delta\mathbf{m}\|_2^2$$
$$\text{subject to} \quad \|\delta\mathbf{d} - \nabla\mathcal{F}\delta\mathbf{m}\|_2^2 \leq \sigma$$

w/ linearized Bregman iterations for $k = \{1,2,\cdots,\text{niter}\}$

$$\begin{aligned} \mathbf{u}^{k+1} &= \mathbf{u}^k - t^k \nabla\mathcal{F}^{k\top}(\nabla\mathcal{F}^k\delta\mathbf{m}^k - \delta\mathbf{d}^k) \\ \delta\mathbf{m}^{k+1} &= \mathbf{C}^\top S_\lambda(\mathbf{C}\mathbf{u}^{k+1}) \end{aligned}$$

- $\mathbf{C}$ curvelet transform, S_λ soft thresholding
- Works on random subsets of shots (inversion cost $(1.5-2)\times$ RTM)

True velocity $\mathbf{m}_j$

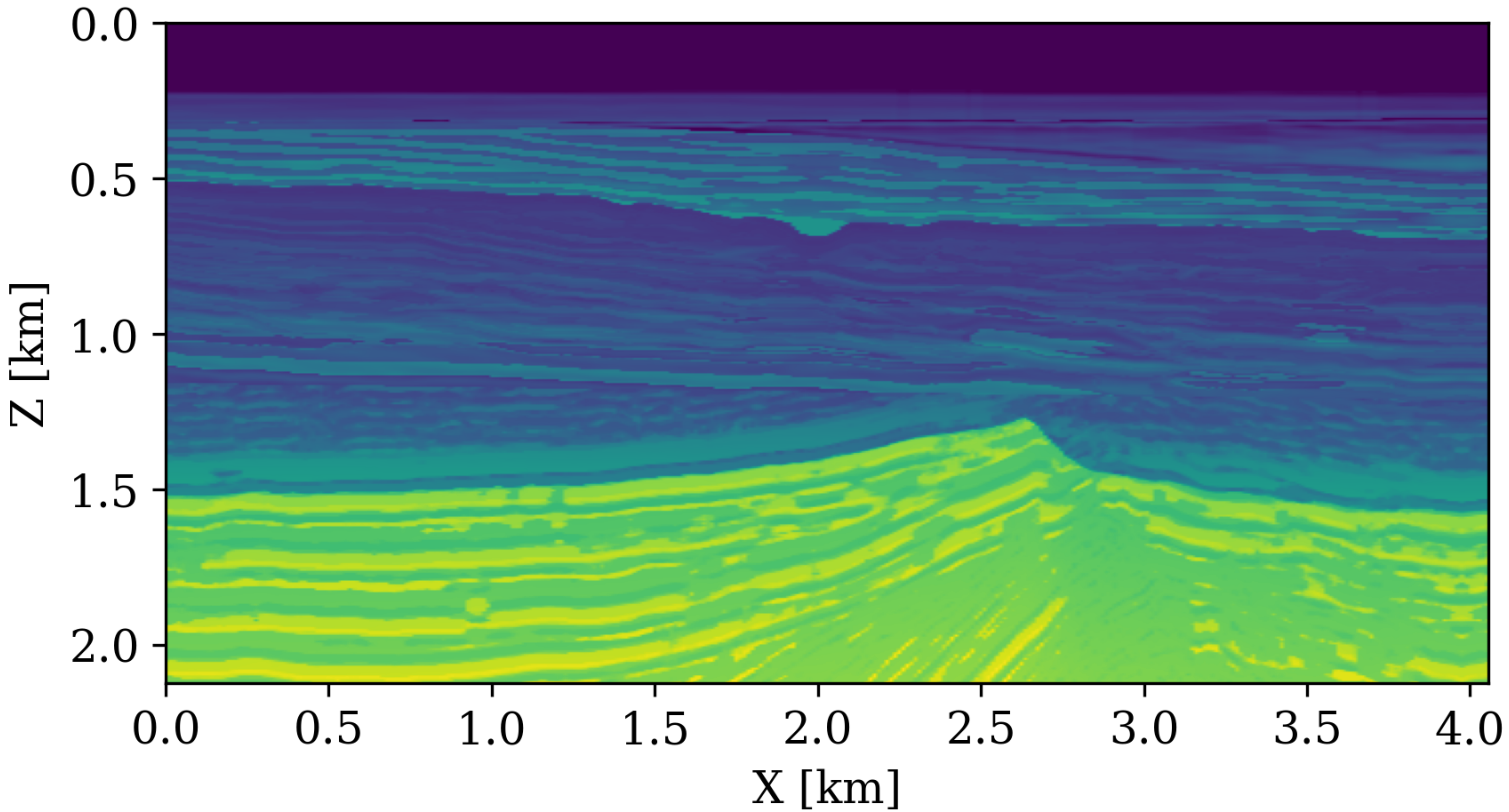

Background velocity $\overline{\mathbf{m}}_j$

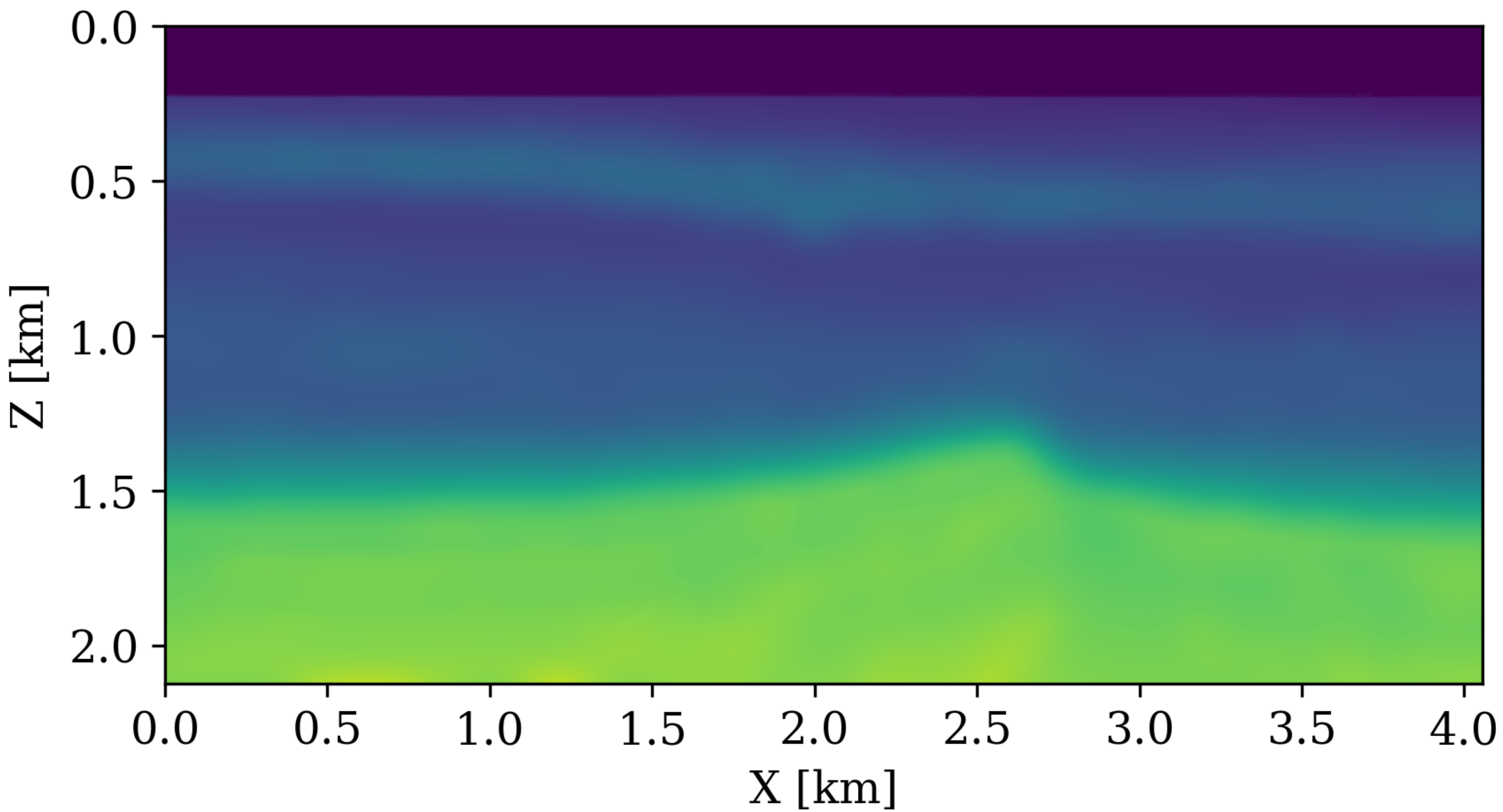

Velocity perturbation $\delta \mathbf{m}_j$

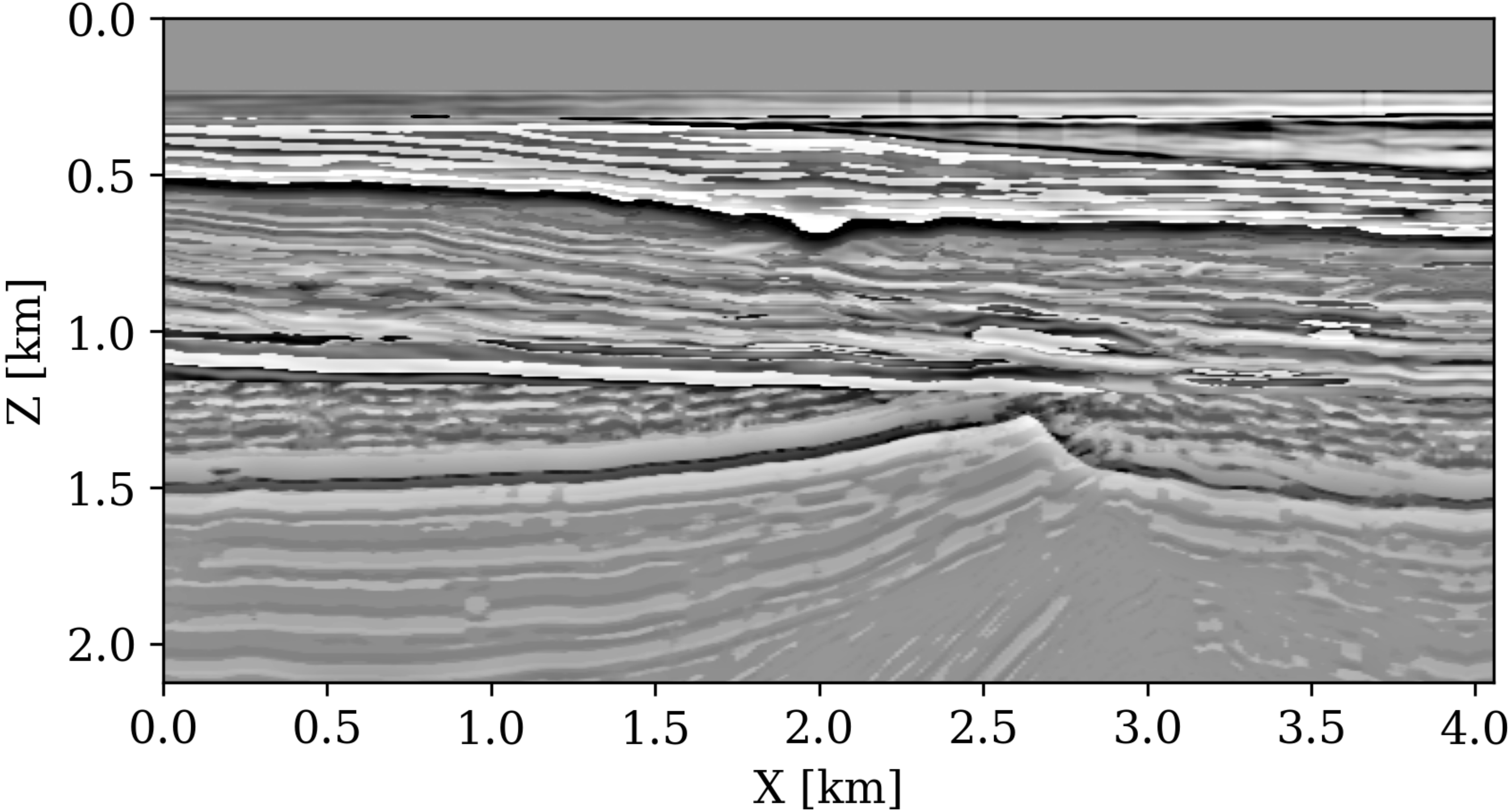

SPLS-RTM on linear data

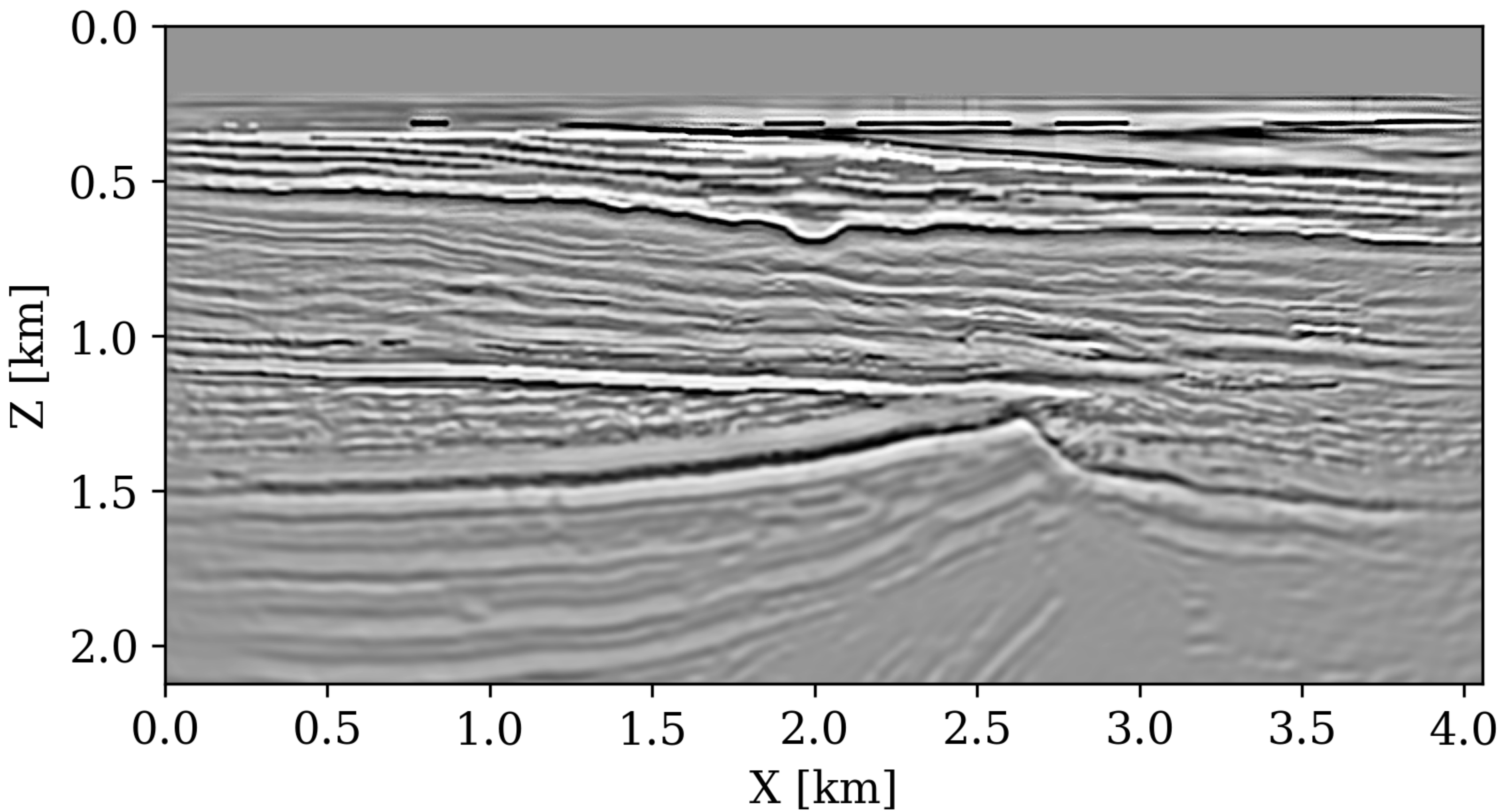

Independent imaging

independent recovery

$$\mathbf{A} = \begin{bmatrix} \nabla\mathcal{F}_1(\overline{\mathbf{m}}_1) & \mathbf{0} & \mathbf{0} & \mathbf{0} \\ \mathbf{0} & \nabla\mathcal{F}_2(\overline{\mathbf{m}}_2) & \mathbf{0} & \mathbf{0} \\ \mathbf{0} & \mathbf{0} & \cdots & \mathbf{0} \\ \mathbf{0} & \mathbf{0} & \mathbf{0} & \nabla\mathcal{F}_{n_v}(\overline{\mathbf{m}}_{n_v}) \end{bmatrix}$$

$$\mathbf{x} = \left[\mathbf{x}_1^\top, \cdots, \mathbf{x}_{n_v}^\top\right]^\top \qquad \mathbf{b} = \left[\delta\mathbf{d}_1^\top, \delta\mathbf{d}_2^\top, \cdots, \delta\mathbf{d}_{n_v}^\top\right]^\top$$

- vintages are not connected to each other
- image-domain coherent artifacts due to non-replicated acquisition, etc., can be wrongly attributed to time-lapse signal

SLIM

Joint Imaging

joint recovery model

New imaging/monitoring paradigm:

- ► time-lapse signal assumed to be “localized”
- ► exploit information shared amongst different vintages
- ► monitoring benefits from differences in acquisition
- ► more robust w.r.t. noise
- ► recover more repeatable images

Felix Oghenekohwo, Haneet Wason, Ernie Esser, and Felix J. Herrmann, "Low-cost time-lapse seismic with distributed compressive sensing–-Part 1: exploiting common information among the vintages", Geophysics, vol. 82, pp. P1-P13, 2017.
Felix Oghenekohwo, Rajiv Kumar, Ernie Esser, and Felix J. Herrmann, "Using common information in compressive time-lapse full-waveform inversion", EAGE, 2015.

SLIM

Joint Imaging

joint recovery model

$$\tilde{\mathbf{A}} = \begin{bmatrix} \frac{1}{\gamma}\nabla\mathcal{F}_1(\overline{\mathbf{m}}_1) & \nabla\mathcal{F}_1(\overline{\mathbf{m}}_1) & \mathbf{0} & \mathbf{0} & \mathbf{0} \\ \frac{1}{\gamma}\nabla\mathcal{F}_2(\overline{\mathbf{m}}_2) & \mathbf{0} & \nabla\mathcal{F}_2(\overline{\mathbf{m}}_2) & \mathbf{0} & \mathbf{0} \\ \cdots & \mathbf{0} & \mathbf{0} & \cdots & \mathbf{0} \\ \frac{1}{\gamma}\nabla\mathcal{F}_{n_v}(\overline{\mathbf{m}}_{n_v}) & \mathbf{0} & \mathbf{0} & \mathbf{0} & \nabla\mathcal{F}_{n_v}(\overline{\mathbf{m}}_{n_v}) \end{bmatrix}$$

$$\mathbf{z} = \left[\mathbf{z}_0^\top, \mathbf{z}_1^\top, \cdots, \mathbf{z}_{n_v}^\top\right]^\top \qquad \mathbf{b} = \left[\delta\mathbf{d}_1^\top, \delta\mathbf{d}_2^\top, \cdots, \delta\mathbf{d}_{n_v}^\top\right]^\top$$

common component ($\mathbf{z}_0$)

innovation component ($\mathbf{z}_1, \cdots, \mathbf{z}_{n_v}$)

Felix Oghenekohwo, Haneet Wason, Ernie Esser, and Felix J. Herrmann, “Low-cost time-lapse seismic with distributed compressive sensing–-Part 1: exploiting common information among the vintages”, Geophysics, vol. 82, pp. P1-P13, 2017.
Felix Oghenekohwo, Rajiv Kumar, Ernie Esser, and Felix J. Herrmann, “Using common information in compressive time-lapse full-waveform inversion”, EAGE, 2015.

SLIM

Forward model

joint recovery model

$$\tilde{\mathbf{A}} = \begin{bmatrix} \frac{1}{\gamma}\nabla\mathcal{F}_1(\overline{\mathbf{m}}_1) & \nabla\mathcal{F}_1(\overline{\mathbf{m}}_1) & \mathbf{0} & \mathbf{0} & \mathbf{0} \\ \frac{1}{\gamma}\nabla\mathcal{F}_2(\overline{\mathbf{m}}_2) & \mathbf{0} & \nabla\mathcal{F}_2(\overline{\mathbf{m}}_2) & \mathbf{0} & \mathbf{0} \\ \cdots & \mathbf{0} & \mathbf{0} & \cdots & \mathbf{0} \\ \frac{1}{\gamma}\nabla\mathcal{F}_{n_v}(\overline{\mathbf{m}}_{n_v}) & \mathbf{0} & \mathbf{0} & \mathbf{0} & \nabla\mathcal{F}_{n_v}(\overline{\mathbf{m}}_{n_v}) \end{bmatrix}$$

$$\mathbf{z} = \left[\mathbf{z}_0^\top, \mathbf{z}_1^\top, \cdots, \mathbf{z}_{n_v}^\top\right]^\top \qquad \mathbf{b} = \left[\delta\mathbf{d}_1^\top, \delta\mathbf{d}_2^\top, \cdots, \delta\mathbf{d}_{n_v}^\top\right]^\top$$

- common component observed & build by all vintages $\Longrightarrow$ improved images
- innovation components will also be well recovered

Comparison

independent vs joint monitoring

Experimental set-up:

- linearized data (inversion prime)
- fixed sparse ocean bottom hydrophones (250m spacing)
- non-replicated dense sources with varying tow-depth (12.5m spacing)
- source-receiver reciprocity
- ultra-low memory gradients w/ random trace estimation

Compare repeatability quantitatively w/ NRMS values

$$NRMS(\mathbf{x}_1, \mathbf{x}_j) = \frac{200 \times RMS(\mathbf{x}_1 - \mathbf{x}_j)}{RMS(\mathbf{x}_1) + RMS(\mathbf{x}_j)}, \quad j = 2, \cdots, n_v.$$

- small NRMS values $\Longrightarrow$ better repeatability

Independent recovery

poor repeatability (NRMS $> 15\,\%$)

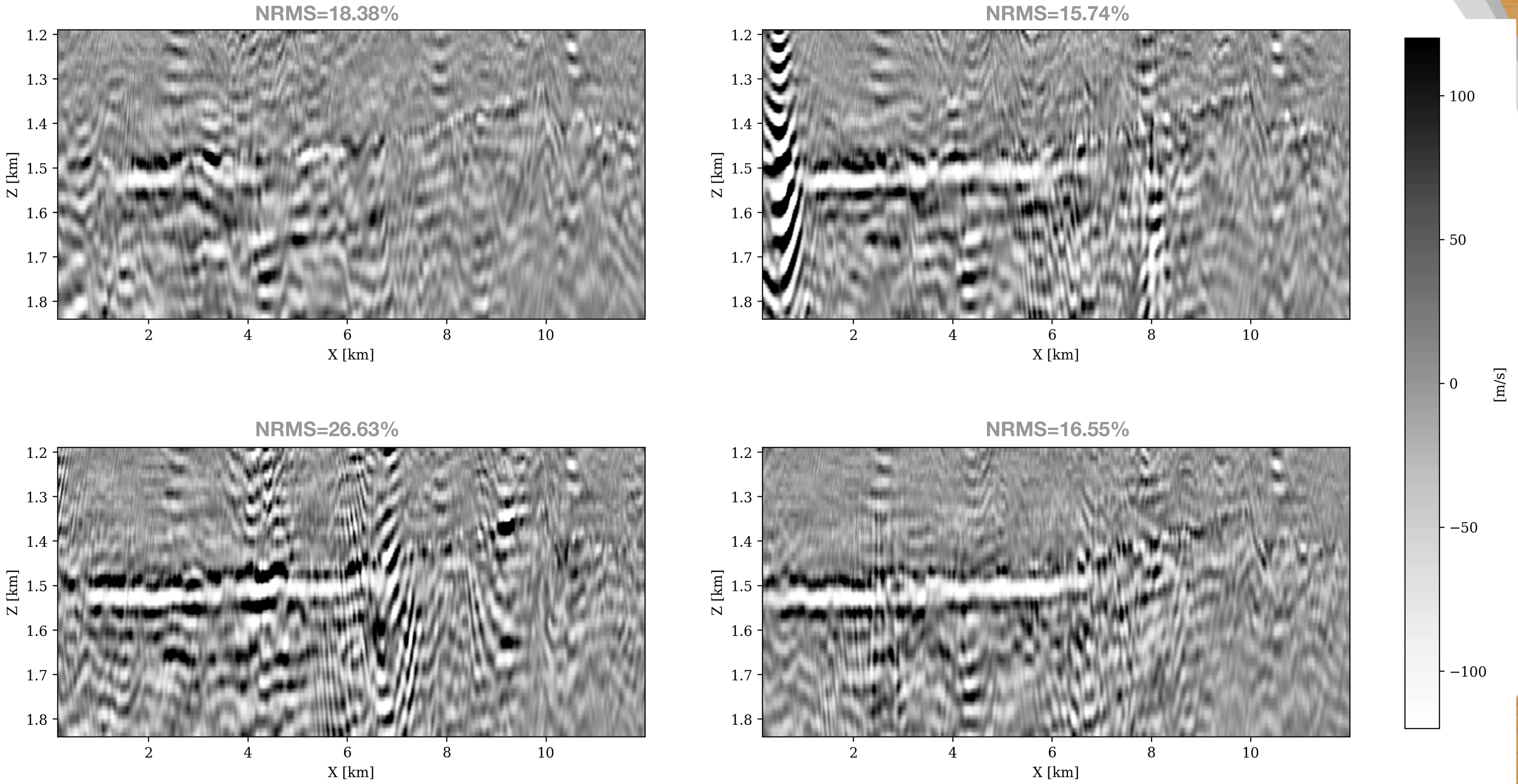

Joint recovery

acceptable repeatability (NRMS $< 10\,\%$)

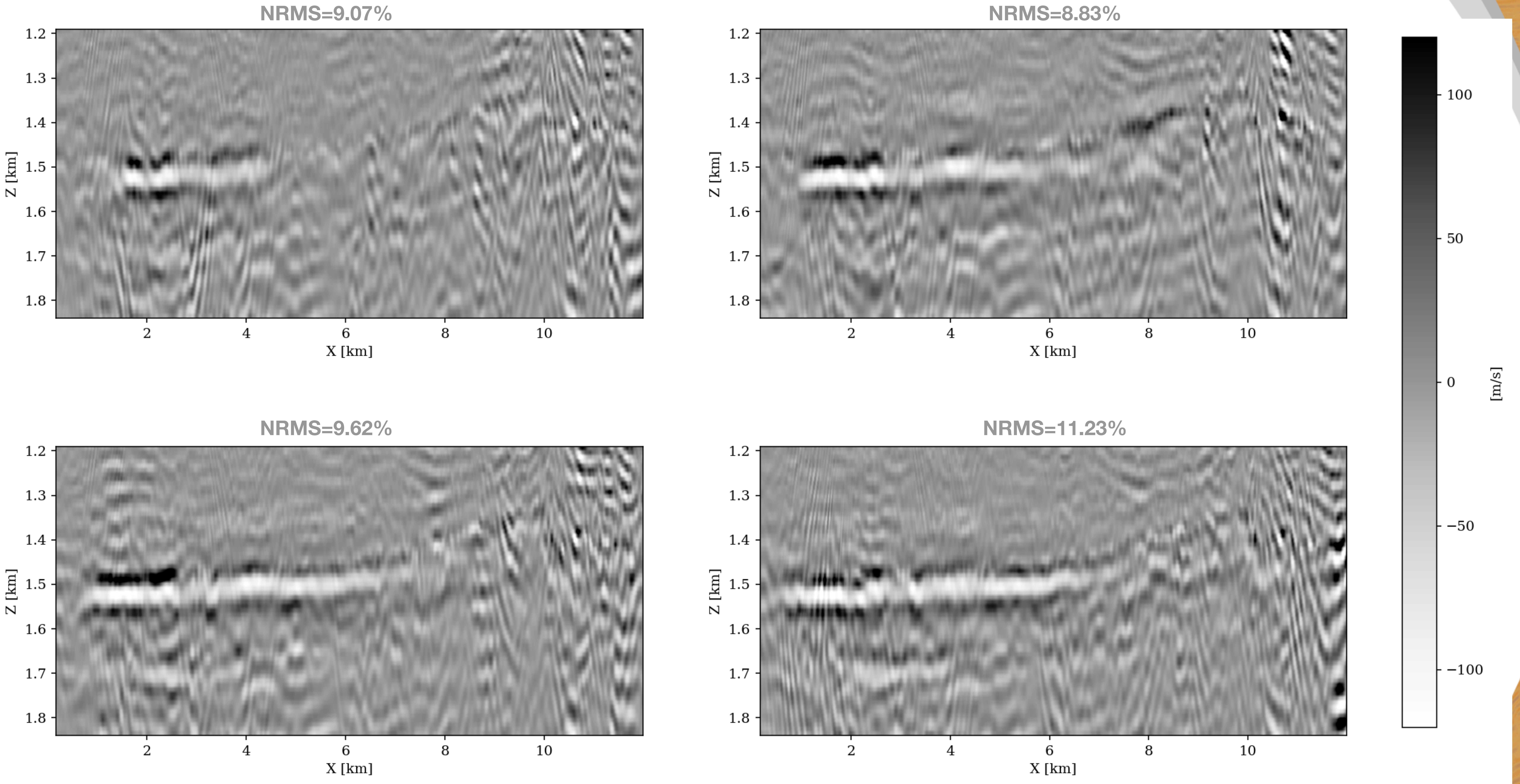

CO_2 plume monitoring

leakage through fault

Synthetic 12-year CCS project

- fault above injection well w/ 12.5m width
- fault opens when pressure exceeds 10^9 Pa
- fault closes after 3 years when pressure drops under 10^7 Pa
- Check seismic detectability

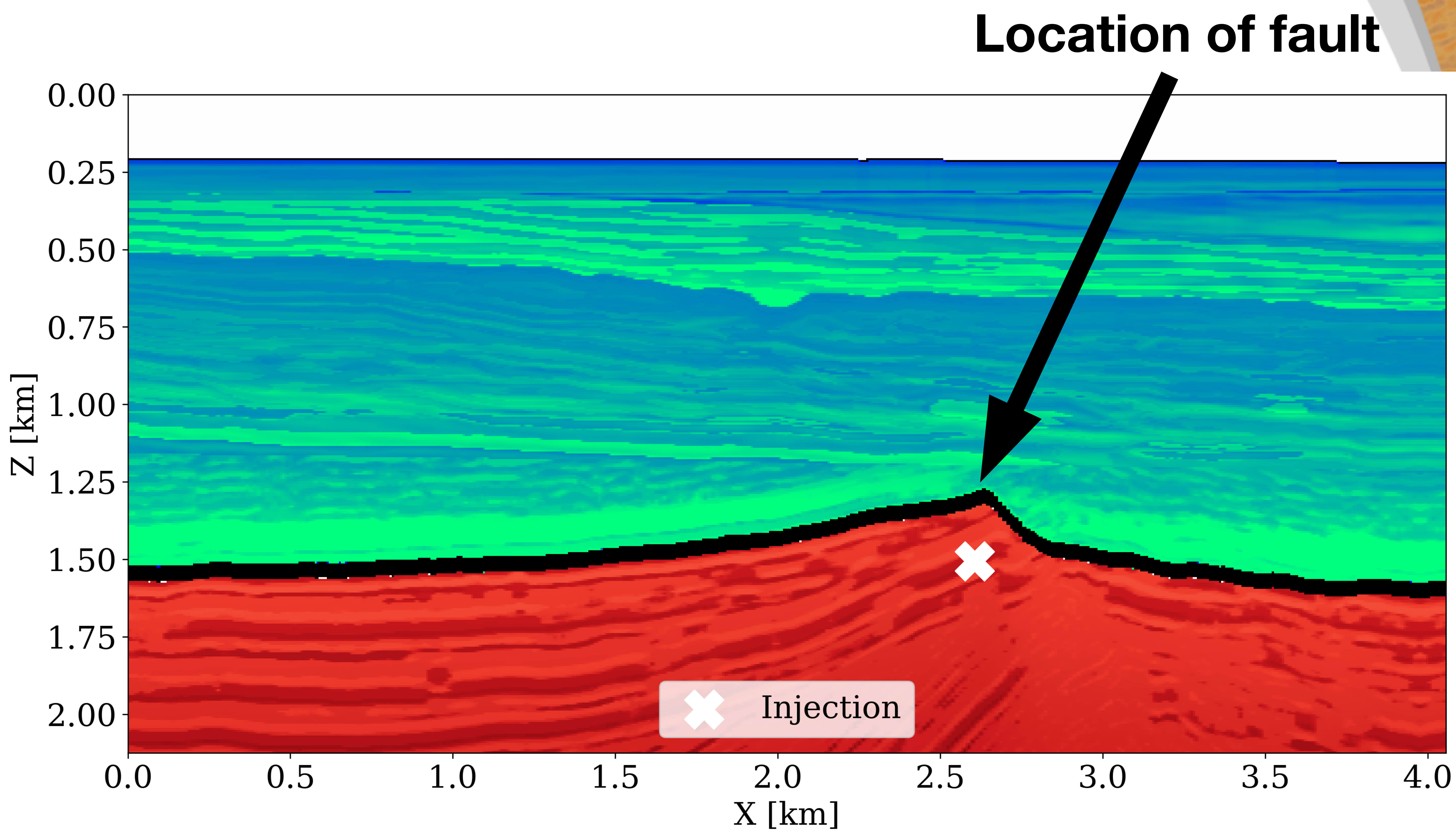

Pressure induced CO_2 leakage

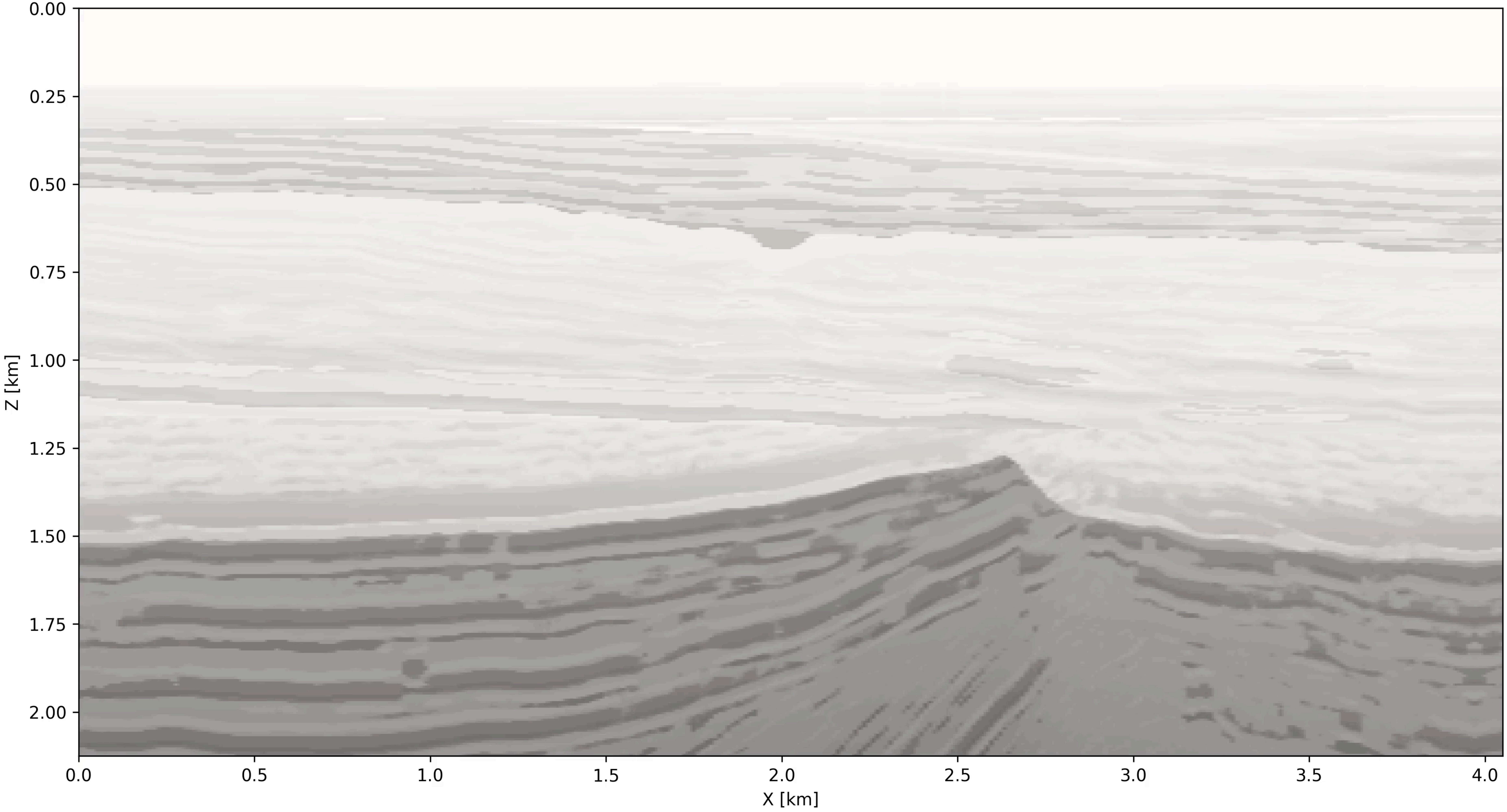

Louboutin, Mathias, and Felix J. Herrmann. "Ultra-low memory seismic inversion with randomized trace estimation." *Accepted by SEG 2021*
Daskalakis, Emmanouil, Felix J. Herrmann, and Rachel Kuske. "Accelerating Sparse Recovery by Reducing Chatter." *SIAM Journal on Imaging Sciences* 13.3 (2020): 1211-1239.
Witte, Philipp A., Mengmeng Yang, and Felix J. Herrmann. "Sparsity-promoting least-squares migration with the linearized inverse scattering imaging condition." *79th EAGE Conference and Exhibition 2017*. Vol. 2017. No. 1. European Association of Geoscientists & Engineers, 2017.

Realistic seismic imaging

Imaging complications:

- free surface multiples — Born modeling w/ free-surface BC
- density variations — inverse scattering imaging condition
- nonlinear data — subtract forward simulation in background model
- inconsistent system — anti-chattering
- incorrect background model at CO_2 plume — focus on top of the plume
- ultra-low memory gradient — approximation w/ random trace estimation
- random noise — joint recovery model

Noisy seismic surveys
band-limited noise (SNR = 0.0 dB)

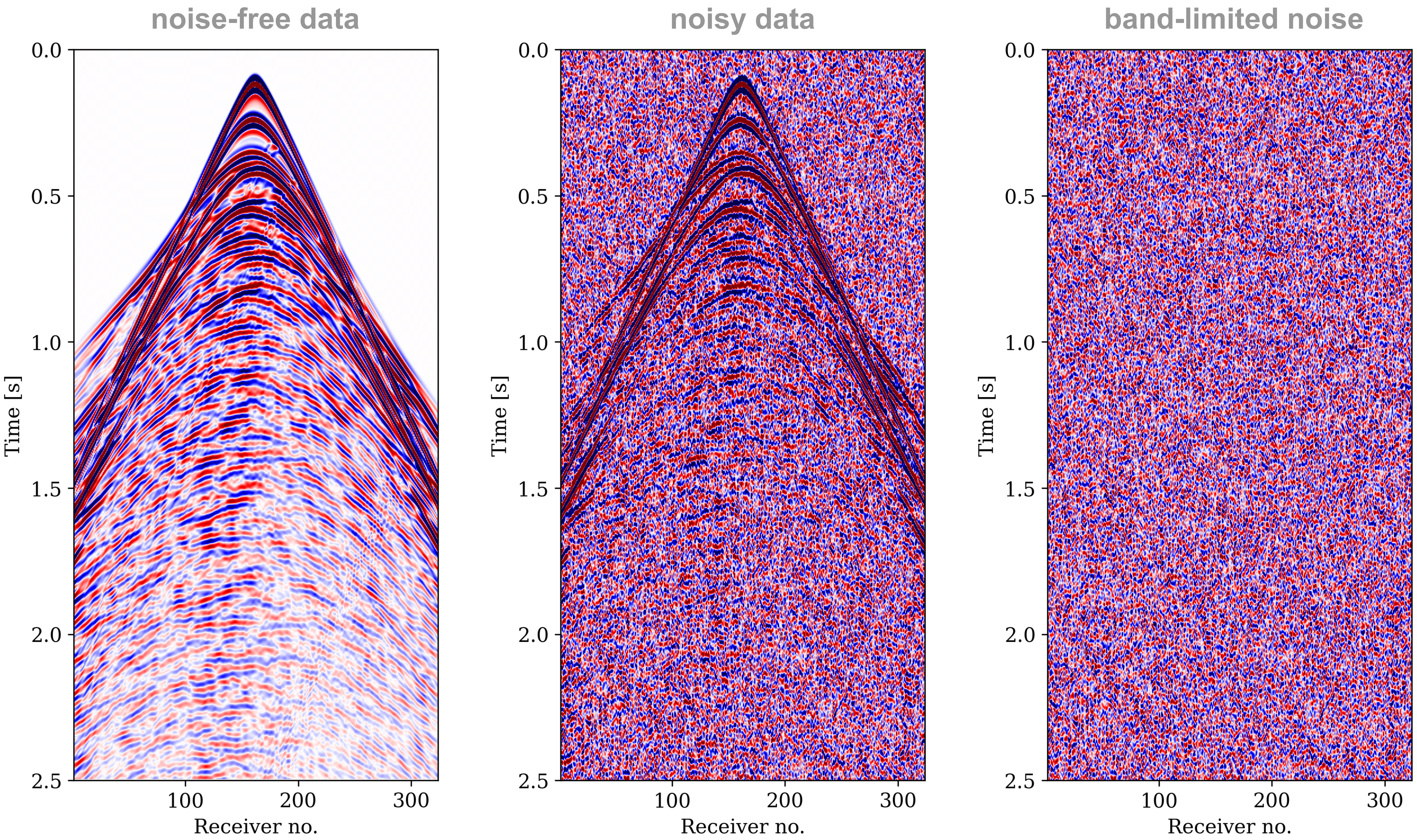

Independent recovery

difference baseline & last monitor survey (NRMS = 26.7%)

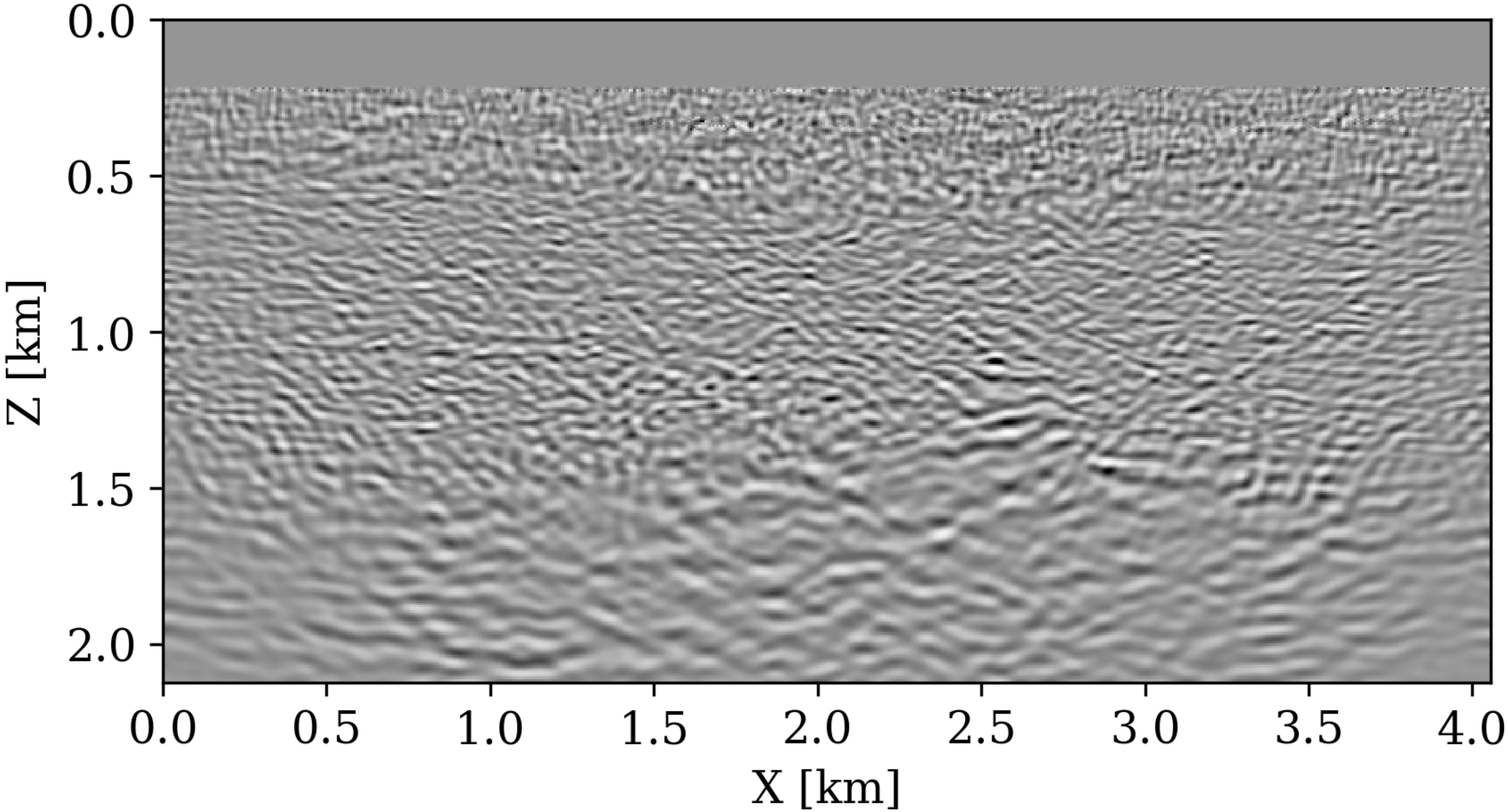

Joint recovery

difference between baseline & last monitor survey (NRMS = 6.92%)

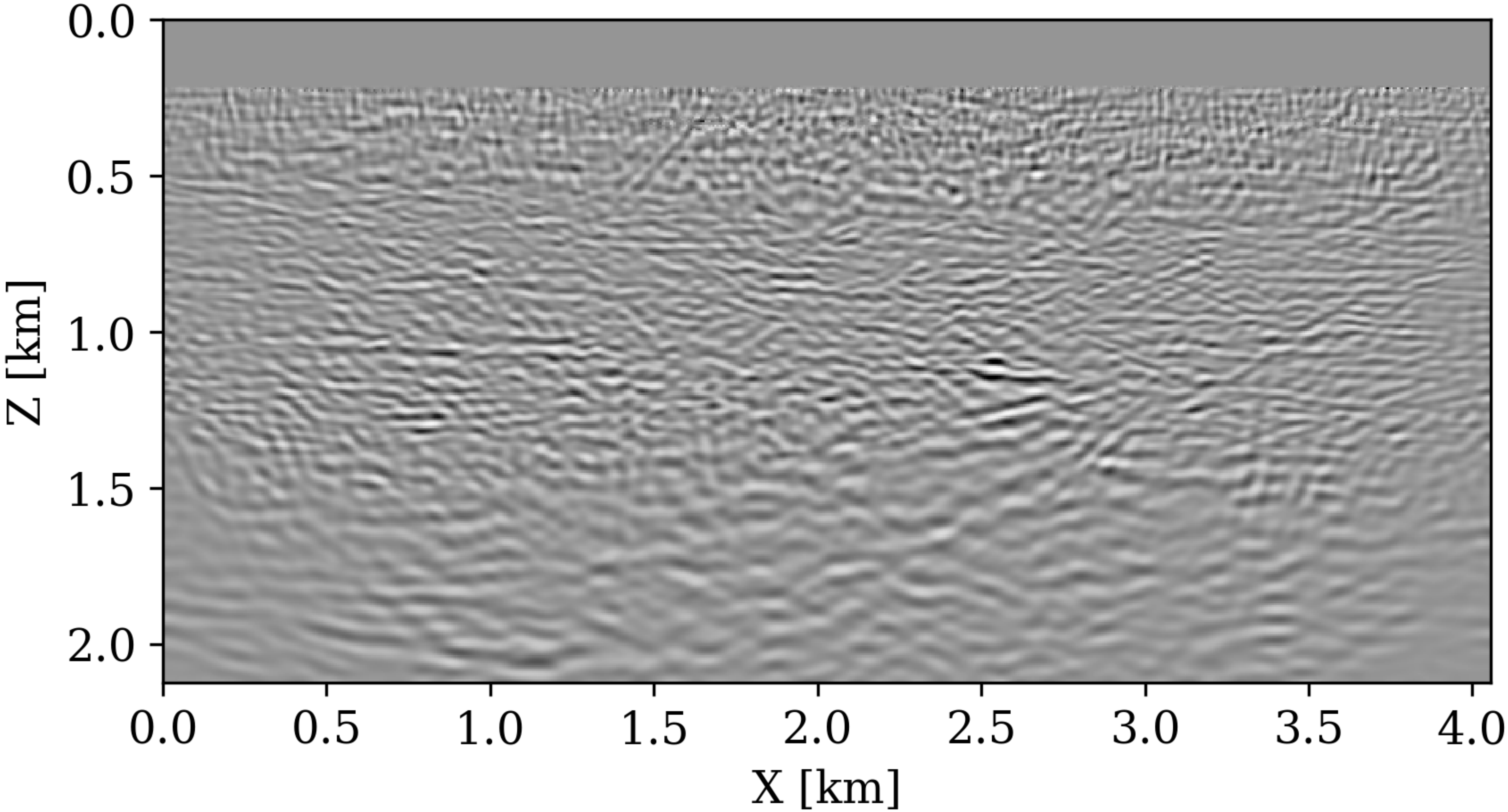

Observations

Low-cost acquisition & imaging scenarios are feasible

Joint recovery model

- improves repeatability w/o insisting on replicating surveys
- robust w.r.t. noise

Working on extension to 3D in collaboration w/ Azure

Part of development open-source framework to

- assess seismic detectability of CO_2 plumes on industry scale
- reduce costs of seismic monitoring systems
- mitigate risk of CCS

Related material

Extension work by Felix J. Herrmann at **W-12 Geophysical Challenges in Presalt Carbonates**

Website https://slim.gatech.edu

We would like to thank the developers of the open-source software packages

- FwiFlow.jl https://github.com/lidongzh/FwiFlow.jl
- Devito https://www.devitoproject.org
- JUDI.jl https://github.com/slimgroup/JUDI.jl
- JOLI.jl https://github.com/slimgroup/JOLI.jl
- TimeProbeSeismic.jl https://github.com/slimgroup/TimeProbeSeismic.jl

Our examples are reproducible located on GitHub at

- https://github.com/slimgroup/Software.SEG2021
- https://github.com/slimgroup/CompassTimeLapseCCS

Acknowledgement

- Thank Charles Jones (Osokey) for the constructive discussion
- The CCS project information is taken from the Strategic UK CCS Storage Appraisal Project, funded by DECC, commissioned by the ETI and delivered by Pale Blue Dot Energy, Axis Well Technology and Costain. The information contains copyright information licensed under ETI Open License.
- This research was carried out with the support of Georgia Research Alliance and partners of the ML4Seismic Center.